Biochemical characterization of two prokaryotic small Ras-like GTPases and their common effector

A thesis submitted towards partial fulfilment of the requirements of BS-MS Dual Degree Program

By

Manil Kanade

20131005

Under the guidance of

Dr. Gayathri Pananghat

Department of Biology

Indian Institute of Science Education and Research (IISER) Pune

Thesis Advisor: **Dr. Nishad Matange,** IISER Pune

Certificate

This is to certify that this dissertation entitled "**Biochemical characterization of two prokaryotic small Ras-like GTPases and their common effector** " towards the partial fulfilment of the BS-MS dual degree programme at the Indian Institute of Science Education and Research (IISER), Pune represents study/work carried out by **Manil Kanade** at the Indian Institute of Science Education and Research, Pune under the supervision of **Dr. Gayathri Pananghat, Assistant Professor, Division of Biology, IISER Pune** during the academic year 2018-19.

Manil Kanade
BS-MS 5th year
20131005

Dr. Gayathri Pananghat
Assistant Professor
Division of Biology IISER Pune

Declaration

I hereby declare that the matter embodied in the report entitled "**Biochemical characterization of two prokaryotic small Ras-like GTPases and their common effector**" are the results of the work carried out by me at the Division of Biology, Indian Institute of Science Education and Research, Pune, under the supervision of **Dr. Gayathri Pananghat** and the same has not been submitted elsewhere for any other degree.

Manil Kanade

BS-MS 5th year IISER PUNE

20131005

Dr. Gayathri Pananghat

Assistant Professor

Division of Biology IISER Pune

Acknowledgements

As I approach the end of my fifth year, I understood if you are determined nothing can stop you from achieving your goals. It a pleasure to express my deepest gratitude to my mentor and guide Dr. Gayathri Pananghat. This project would have not possible without her guidance and support at every step. She is always ready to help with both personal and professional problems. I would like to thank Dr. Saikrishnan Kayarat for his constant support and valuable insights during the project. I thank Dr. Nishad Matange for his valuable insights and being my TAC member. Special thanks to Dr. Rakesh Joshi (IBB Pune) for helping me in MST experiments.

I would like to thanks Jyoti Baranwal, Sukanya Chakraborty, Birjeet, Priyanka Gade, Sonal Lagad and Jazleena PJ for their constant support and preceding work carried in these projects. I thank Manasi, Neha, Mahesh, Ishtiyaq, Mrinmayee, Joyeeta, Pratima, Sutirtha, Vinayak, Vani, Sanket, Karthik, Vishal, Basila, Shrikant and Sujata for maintaining an enjoyable environment for working and helping me during these four years. I want to thank Rupam (JBU lab) for helping me perform mass-spectroscopy. Thanks to my best friends Shamita and Apurva for their constant support and making these years memorable. I would like to thank all my friends at IISER Pune, for making this journey memorable and helping me to learn many things. Finally, I would like to thank my parents and brother for being the best support system an individual could have.

Abstract

Dynamic cell polarity is crucial for many cellular activities. In *Myxococcus xanthus* MglA, a small Ras-like GTPase, and MglB, its GTPase activating protein (GAP), along with RomR (response regulator domain) establish and regulate cell polarity. Recently another small Ras-like GTPase SofG was discovered, which is critical for polar localization of PilB and PilT, the proteins required for pili localization at the leading pole. Both SofG and MglA work in synchrony to drive cell polarity in *Myxococcus xanthus.* Towards understanding the molecular mechanism of SofG action, purification of SofG was optimized, and biochemical characterization was carried out. SofG was present as a homogenous monomer in solution and bound to GDP and GTP. Intrinsic GTP hydrolysis of SofG was negligible. Based on sequence analysis, we hypothesized that MglB could potentially act as a GAP for SofG too, and experimentally showed that MglB increases the GTPase activity of SofG. Earlier work from the lab revealed that MglB functions both as a GAP and a guanosine nucleotide exchange factor (GEF) for MglA. However, our results showed that MglB did not function as a GEF for SofG and did not interact with it in the GDP-bound conformation. The presence of a common GAP for both SofG and MglA could potentially contribute to concerted regulatory mechanisms of their GTPase activities, and mediate crosstalk between the two GTPases within the cell.

Our sequence analysis of the MglB interacting interface also led to the discovery of a novel catalytic motif in prokaryotic small Ras-like GTPases. Interestingly, the Walker B aspartate, thought to be absent in prokaryotic small Ras-like GTPases, was located within this newly identified motif. This was further validated experimentally by mutational analysis and GTPase activity measurements.

Table of Contents

Chapter 3. Results

List of Figures

List of tables

Chapter 1. Introduction

1.1 Small Ras-like GTPase

An extensive family of small Ras-like GTPases performs a wide range of functions from cell polarity to cellular motility (Wittinghofer and Vetter, 2011). GTP bound form is considered as active while GDP bound is inactive (Bourne et al.1998). Small GTPases shuffle between active and inactive forms, which enables them to function as molecular switches for cellular processes. GTP bound form interacts with effector proteins and activates downstream signaling cascade (Bishop and Hall, 2000; Hall, 1998). Small GTPases have a higher affinity for GDP. In order to achieve an active state, GDP has to be displaced with GTP. GEF (guanine nucleotide exchange factor) reduces GDP affinity and facilitates binding of GTP, which is more abundant in the cell (Cherfils and Zeghouf, 2013; Vetter and Wittinghofer, 2001; Wittinghofer and Vetter, 2011; Wu et al., 2011). Intrinsic GTP hydrolysis of small GTPases is very slow. For rapid inactivation, GAPs (GTPase activating protein) are required. They enhance GTP hydrolysis by several folds. GAPs and GEFs function in concert to achieve optimal GTP hydrolysis of GTPases (Figure 1.1; (Bos et al., 2007; Mishra and Lambright, 2016).

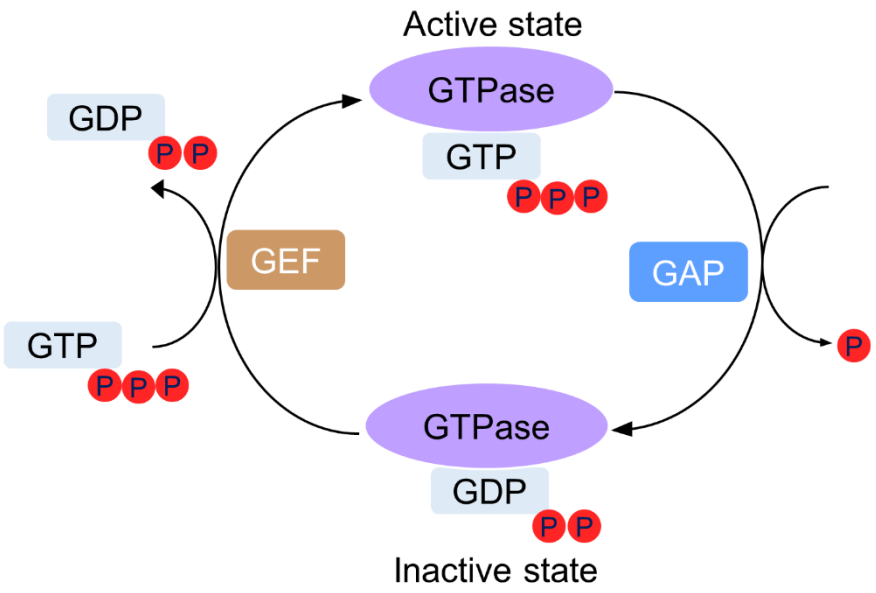

Figure 1.1. GTPase regulatory cycle

Small Ras-like GTPase superfamily is ubiquitous in eukaryotes. This superfamily was further divided into several families and subfamilies on the basis of function, sequence, and structure (Colicelli, 2004; Leipe et al., 2002). Five major families are Ras, Rho, Rab, Ran, and Arf (SAR). Ras family members mainly play a significant role in signal transduction (Rajalingam et al., 2007; Simanshu et al., 2017). Rho GTPase family contains well-studied members like CDC42 and Rac, which are involved primarily in cytoskeleton dynamics and cell polarity (Bishop and Hall, 2000). Rab and Arf family members control intracellular vesicle trafficking. Ran family proteins are most abundant inside the cell, and they regulate nucleo-cytoplasmic transport of proteins and RNA (Li et al., 2003; Takai et al., 2001).

1.2 Structural and sequence features of small Ras-like GTPases

The fundamental G-domain of Ras-like GTPase is a 20-kDa globular protein comprising six beta strands (β1- β6) enclosed by five alpha helices (α1- α5) (Wittinghofer and Vetter, 2011). Although they share low sequence homology, the motifs for GTP binding and hydrolysis are highly conserved (Mishra and Lambright, 2016). As mentioned earlier, the binding of effector proteins to GTPases is dependent on the conformation driven by different nucleotide states. The unique structural and sequence elements of G-proteins ensure the specificity for guanine base, GTP hydrolysis and the release of GDP (Cherfils and Zeghouf, 2013).

The Walker A motif (G1 motif), GxxxxGK[TS] is a unique feature of NTP binding proteins. Since it is essential for stabilization of β, γ-phosphates, this is also termed as P-loop (phosphate-binding loop) (Goitre et al., 2014). The [NT]KxD (G4 motif) and xAx (G5 motif) together determine the specificity for guanine base binding. The aspartate side chain is involved in forming bifurcated hydrogen bonds with guanine whereas alanine creates the main chain interaction to the O6 of guanine. The α1–β2 loop (switch I) and β3–α2 loop (switch II) regions undergo noticeable conformational changes during GTP-GDP transition. The well-ordered switch regions in GTP bound form becomes flexible upon GTP hydrolysis (Gerwert et al., 2017). G2 motif, xTx conserved threonine (part of switch I) stabilize the γ phosphate of GTP and also coordinates with Mg^{2+}. G3 motif DxxGQ is essential for GTP hydrolysis. The conserved glutamine forms water-mediated interaction with the γ phosphate of GTP. Aspartate is

also considered as the Walker B motif and is involved in water-mediated magnesium co-ordination (Mishra and Lambright, 2016; Wittinghofer and Vetter, 2011).

1.3 Common mechanism of GAP stimulation

The function of GAP is to enhance GTP hydrolysis. In contrast to GTPases, GAPs do not have a conserved fold or signature motif. Glutamine and arginine are primary catalytic residues for GTP hydrolysis. In the transition state negative charge of γ-phosphate is stabilized by arginine finger. GAPs often provide the arginine finger. In some instances, this arginine is present intrinsically, and GAP helps in positioning the residue for active hydrolysis. Glutamine is intrinsically present in the GTPase, in most cases. Glutamine orients the catalytic water to facilitate an attack on γ-phosphate. GAP re-orients glutamine (Cherfils and Zeghouf, 2013; Gerwert et al., 2017; Mishra and Lambright, 2016).

1.4 Common mechanism of GEF stimulated exchange reaction

Small GTPases generally have high affinity to GDP, since GDP dissociation is very slow. GEF accelerates GDP dissociation by reducing the GDP affinity. This can be achieved by different mechanisms. Some of them are as follows: i) inducing a conformational change in switch I and switch II (Qiu et al., 2014; Wu et al., 2011) ii) reducing the guanine specificity iii) destabilizing the phosphate loop (Miyamoto et al., 2007). GEFs stabilize nucleotide-free state of GTPase till new GTP binds. GTP binding will eventually dissociate the GEF from GTPase (Cherfils and Zeghouf, 2013).

1.5 *Myxococcus xanthus* as a model system to study bacterial cell polarity

Cell polarity is an asymmetric organization of different components, which includes cell surface, cytoskeleton and protein distribution. Cell polarity is ubiquitous and observed in prokaryotes and eukaryotes (Davis and Waldor, 2013). In eukaryotes, cell polarity and motility are achieved by intricate communication between small Ras-like GTPases and cytoskeleton system (Iden and Collard, 2008). How bacterial cell polarity is established, and its regulation is still not fully known. It was known that bacteria sort proteins, which was traditionally thought to be diffusion dependent. Recent studies on multiple organisms suggested that bacteria are highly organized and regulated.

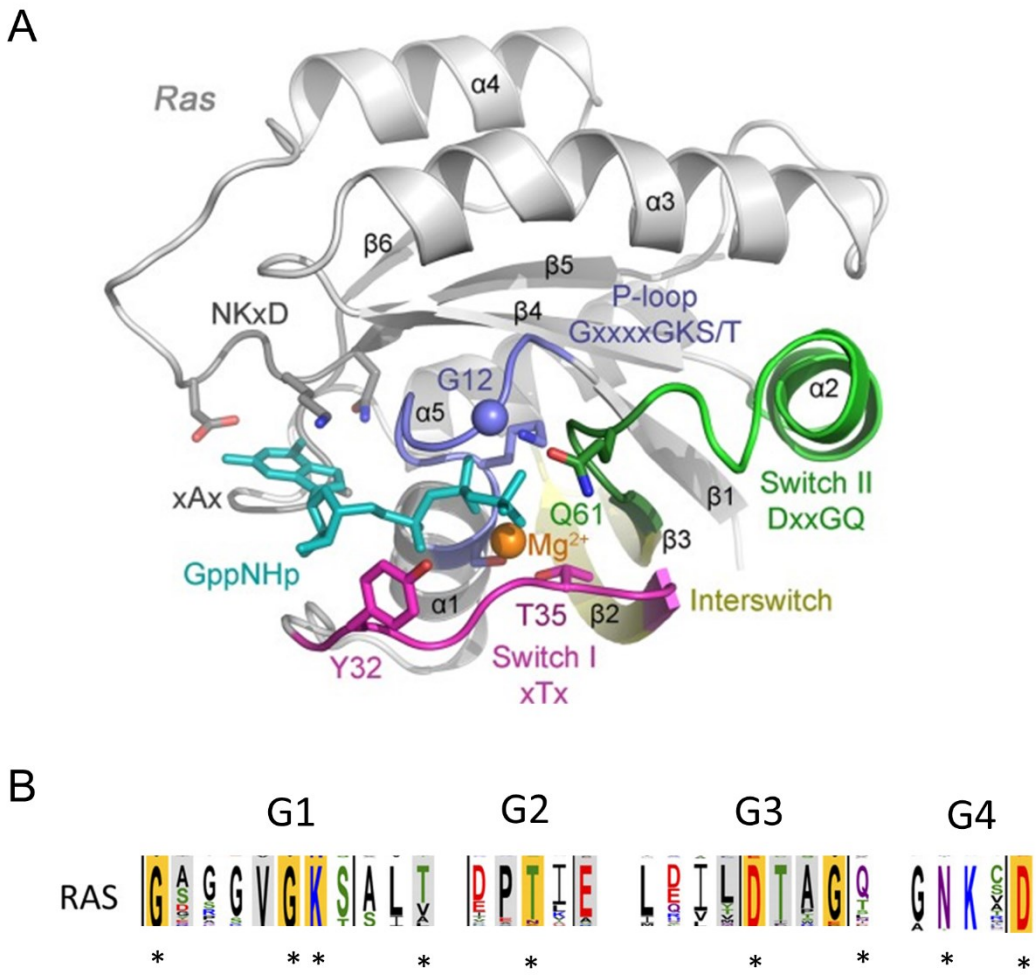

Figure: 1.2 Structural features of Ras-like GTPase

A. Structure of H-Ras bound with GppNHp (PDB ID 5P21). Key functional residues are shown in sticks. Distinctive G motif and switch regions are indicated as follows: G1 motif (blue), Switch and G2 (magenta), Switch II and G3 (green) and G4 (grey), adapted from (Mishra et al, 2013) **B.** Conservation of G1 – G4 motifs in eukaryotic small Ras-like GTPases, adapted from (Rojas et al, 2012)

Bacterial cell polarity is highly dynamic in contrast to what was earlier hypothesized to be static and diffusion dependent and can change in response to external signals. Bacterial cell polarity provides a basis for numerous cellular processes like cell growth, signal transduction, cell division and cellular motility (Schumacher and Søgaard-Andersen, 2017). Because of its fascinating cellular reversals and multifaceted motility machinery, *Myxococcus xanthus* has served as one of the ideal systems to understand cell polarity and motility in bacteria.

Myxococcus xanthus is a soil bacterium, which glides on solid surface (Hartzell and Kaiser, 1991). *Myxococcus xanthus* gliding relies on two distinct motility machinery i) social motility (S-motility) driven by Type IV pili (T4P) and ii) adventurous motility (A-motility) which is facilitated by focal adhesion-like protein complexes (Schumacher and Søgaard-Andersen, 2017).

S-motility is generally dependent on cell-cell contact; the mechanistic details of this machinery is analogous to the twitching motility of *Pseudomonas* and *Neisseria* (Schumacher and Søgaard-Andersen, 2017). S-motility is achieved by extension, adhesion to the solid surface and retraction of T4P, which helps bacteria to move in the forward direction. The cytoplasmic ATPases of AAA+ family PilB and PilT associate at the base of T4P and drive extension and retraction respectively (Jakovljevic et al., 2008).

A-motility has many parallels with eukaryotic cell crawling. Isolated cells move individually; hence this motility is called as adventurous motility. Attachment and detachment of focal adhesion-like protein complexes to the substratum generate a force which facilitates gliding to the solid surface (Faure et al., 2016). PMF (proton motive force) provides energy for active propulsion through the action of the motor proteins MotA and MotB (Fu et al., 2018).

Cell polarity plays a vital role in the regulation of both motilities. Motility complexes have been found asymmetrically localized at cell poles while some polarity complexes are distributed across cells. Presence of T4P determines leading and lagging pole of the cell. The pole where T4P are present is considered as the leading pole, while the other pole is the lagging pole (Zhang et al., 2012). *Myxococcus xanthus* also undergo frequent reversals, which play a vital role in determining the direction of movement. Reversals are regulated by Frz chemosensory pathway (Kaimer et al., 2012).

1.6 MglA and MglB proteins establish leading and lagging poles

Earlier genetic studies on *Myxococcus xanthus* led to the discovery of mutual gliding operon consisting of two genes *mglA* and *mglB*. Deletion of these genes affected both

motilities in *Myxococcus xanthus* (Hartzell and Kaiser, 1991). Further biochemical studies implicated that *mglA* gene encodes for a small Ras-like GTPase MglA, and *mglB* gene encodes its cognate GTPase activating protein MglB (Zhang et al., 2010). MglA structure is closer to Arf family of eukaryotic small Ras-like GTPases, while MglB possesses roadblock domain (Miertzschke et al., 2011). Roadblock domain is similar to eukaryotic longin domain. Structural analysis suggested that roadblock domain-like fold serves as a platform that forms an interaction interface for the small Ras-like GTPase (Levine et al., 2013).

MglA and MglB along with RomR (a response regulator domain) establish and maintain polarity essential for both motilities (Keilberg and Søgaard-Andersen, 2014). MglA binds to both GTP and GDP, and intrinsic GTP hydrolysis is very slow. MglA-GTP (active form) is localized at the leading pole, while MglA-GDP (inactive form) is distributed in the cytoplasm. Presence of MglA-GTP at the leading pole is essential for the assembly of the A-motility apparatus (Zhang et al., 2010). RomR is essential for polar localization of MglA-GTP.

MglA/B establishes dynamic cell polarity in *Myxococcus xanthus* (Figure 1.3 A). Initially, MglA-GTP is localized symmetrically at both poles. MglB generates asymmetry by converting MglA-GTP to MglA-GDP at one of the poles. MglA-GTP is distributed asymmetrically. T4P assemble at the pole where local concentration MglA-GTP is high, considered as the leading pole. MglB is present at lagging pole. During reversals, MglA and MglB dissociate from their corresponding poles and associate at the opposite poles, leading to polarity inversion (Figure 1.3 B) (Keilberg and Søgaard-Andersen, 2014; Schumacher and Søgaard-Andersen, 2017). To summarize, MglA and MglB module establishes cell polarity in *Myxococcus xanthus.*

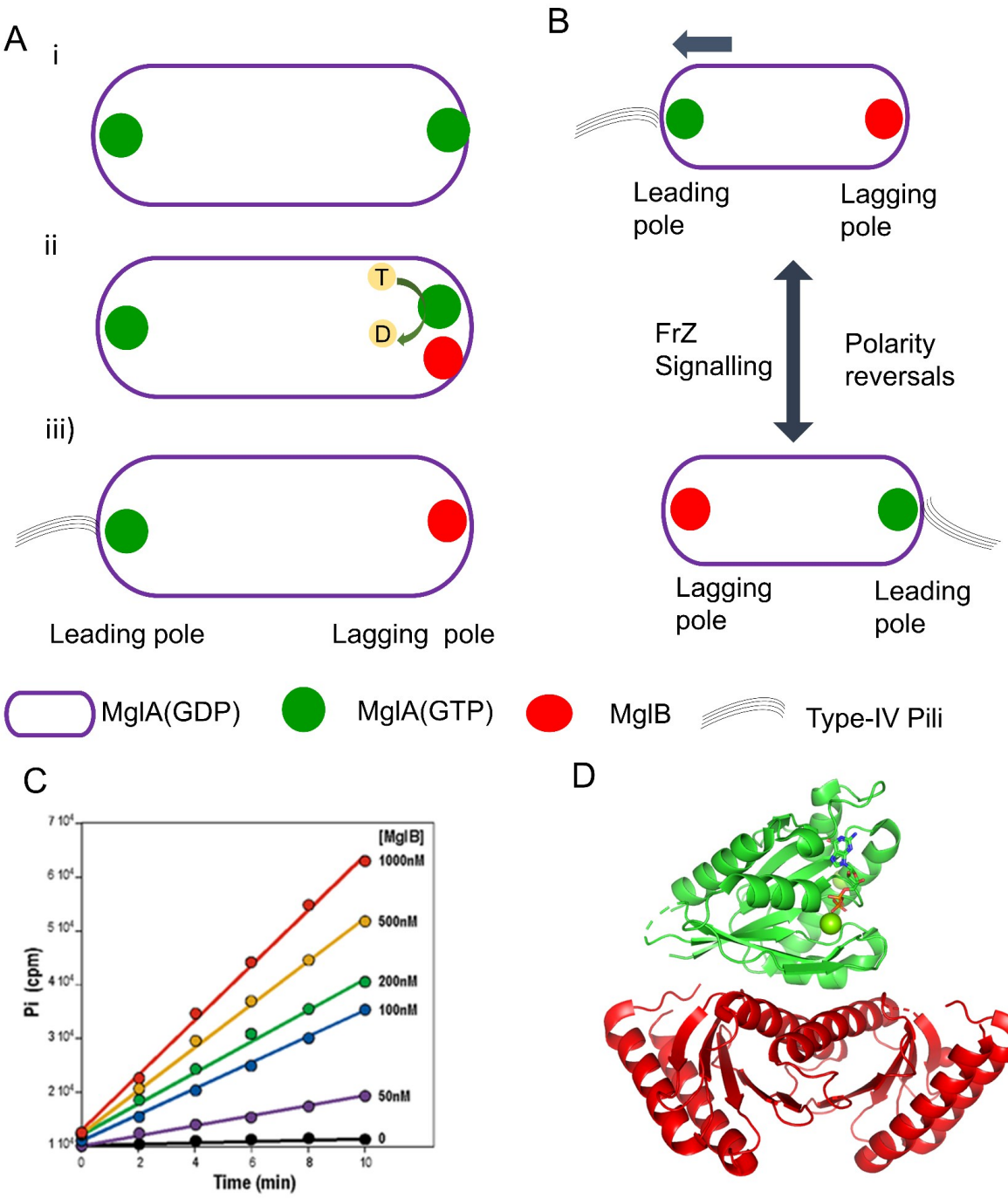

Figure 1.3. MglAB module is essential for cell polarity regulation in *M. xanthus.*

A. MglA and MglB establish cell polarity (details explained in text). **B.** Schematic representation of polarity reversals induced by Frz signalling **C.** MglB is a GAP for MglA GTP hydrolysis assay with increasing concentration of MglB demonstrates (adapted from Zhang, et al, 2010). **D.** *Thermus thermophilus* MglA and MglB complex structure in presence of GppNHp (PDB: 3T1Q). MglA interacts with a dimer of MglB (1:2).

1.7 SofG drives polar localization of PilB and PilT

Recent studies discovered another novel small Ras-like GTPase protein in *Myxococcus xanthus*. Since deletion of this protein affected S-motility in the bacterium, this protein was named as SofG (Social motility function GTPase). SofG is a MglA paralog, which shares 45 % sequence identity with MglA (Figure 1.4). SofG has four signature G-domain motifs; it also has the intrinsic arginine finger like MglA. In contrast to MglA, SofG has an extra C-terminal domain (Bulyha et al., 2013). Further, it was also found that SofG is essential for T4P assembly. SofG interacts with Bactofilin P (BacP) filament and the interaction is necessary for the proper functioning of SofG. As mentioned earlier, PilB and PilT drive extension and retraction of T4P. SofG is vital for polar localization of PilB and PilT. In the absence of SofG, PilB and PilT are present in the subpolar region of the cells. Based on these initial observations, a model was suggested for the action of SofG (Figure 1.5). The steps for the process include: a) Bactofilin P filament is localized at both the cell poles, SofG interacts with BacP at one of the poles (subpolar localization) b) PilB and PilT interact with SofG c) active GTP hydrolysis drives shuttling of SofG over BacP to localize PilB and PilT at one of the cell poles d) MglAB protein module then sorts PilB and PilT in opposite poles. Thus MglA and SofG work in concert to achieve cell polarity in *Myxococcus xanthus* (Bulyha et al., 2013).

Figure 1.4. Sequence alignment of *Myxococcus xanthus* SofG and MglA. Conserved G-motifs are highlighted.

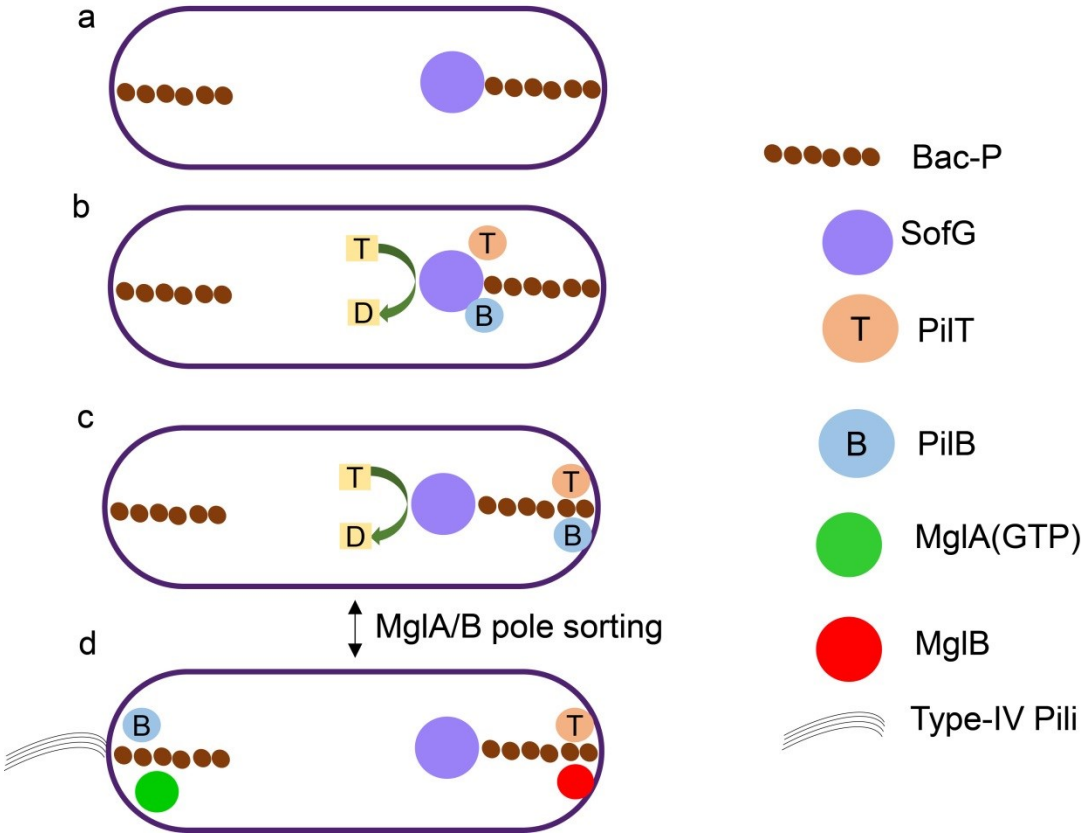

Figure 1.5 Proposed model for function of SofG and BacP in regulation of cell polarity in *Myxococcus xanthus.*

1.8 Structural insights into the MglA/B module

To understand the molecular mechanism of MglA and MglB module, biochemical and structural studies of *Myxococcus xanthus* MglA and MglB were initiated in the lab (Baranwal, Ph.D. thesis, 2019). MglAB complex structure in the presence of GTP analog discovered a novel interaction of C-terminal helix of MglB with α5 helix of MglA. Interestingly MglB interacted with MglA in both GDP and GTP bound forms, while $MglB^{Ct}$ (deletion of C-terminal helix which interacted with MglA α5 helix) only interacted with the GTP-bound MglA. MglB C-terminal also contributed to GEF activity. Corroborative in vivo studies displayed role of C-terminal helix in regulating cell polarity (Baranwal et al. unpublished).

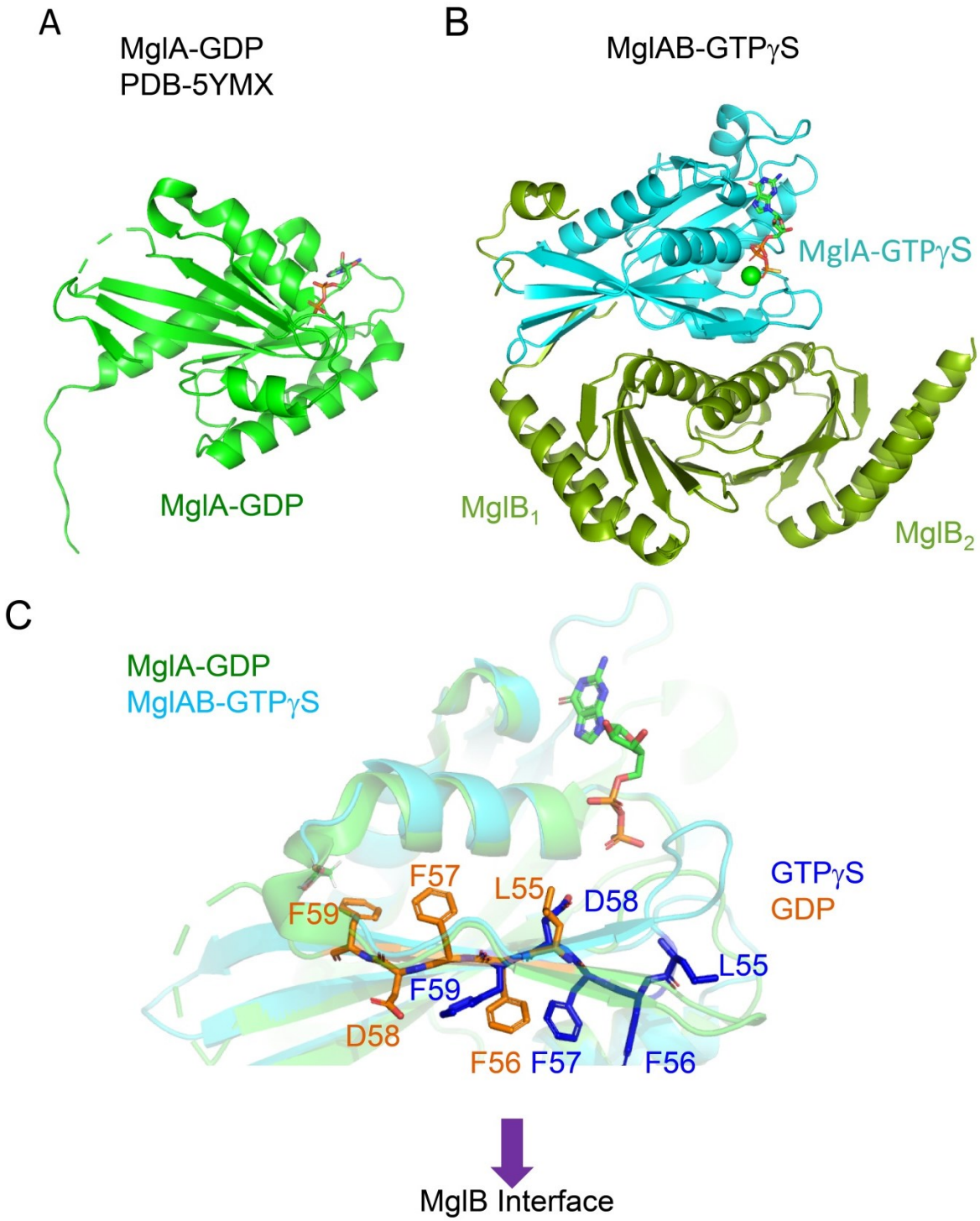

Figure 1.6. Crystal structure of *Myxococcus xanthus* MglA and MglB complex

A. Structure of MglA bound to GDP (green) **B.** Structure of MglA (cyan) in complex with MglB (green) in presence of GTPγS (PDB ID 6IZW) **C.** β screw rotation observed in MglA. Comparison of MglA-GDP (green) and MglA-GTPγS (cyan). Residues in β2 strand are shown in sticks for MglA-GDP (orange) and MglA-GTPγS (blue).

Comparison of *Myxococcus xanthus* MglA-GDP and MglAB complex structures demonstrated conformational changes in MglA accompanying MglB binding. These include optimal orientation of active site residues Arg54 and Gln82, and β-strand flipping (β-screw movement) which exposes hydrophobic residues of MglA towards MglB, thus facilitating MglB binding. These changes were also observed in *Thermus thermophilus* MglAB complex structure. Biochemical studies also suggested that β-strand flipping is important for MglAB complex formation.

1.9 Rationale behind the study

Small Ras-like GTPase switches are emerging as significant players for cell polarity regulation in *Myxococcus xanthus*. Small GTPases are widespread in the bacterial kingdom, but their function is not known. *Myxococcus xanthus* can serve as a model system to understand how multiple GTPases cross-talk and regulate cellular processes.

An intricate network of small GTPases perform various cellular processes in eukaryotes, and due to their functional redundancy and complexity, understanding their role and mechanism of action becomes challenging. In contrast to eukaryotes, the *Myxococcus* cell polarity module consists of two small Ras-like GTPases acting in concert to modulate cell polarity. Hence, this serves as an ideal system to characterise the molecular mechanism of concerted action of GTPases in cell polarity determination.

1.10 Objectives

The primary focus of my project is to understand molecular mechanism of prokaryotic small Ras-like GTPases in *Myxococcus xanthus* using structural and biochemical approaches.

Major objectives of my project include:

- Purification optimization of SofG
- Biochemical characterization SofG
- Mutational analysis of MglA and MglB to understand their nature of interaction
- Sequence analysis of prokaryotic small Ras-like GTPases and their associated MglB sequences

The following chapters in the thesis include a detailed description of the methods, the results obtained and interpretations and significance of the observations.

Chapter 2. Materials and Methods

This chapter describes different experimental methods used in the thesis.

2.1 Cloning

All constructs were made using restriction-free (RF) cloning strategy (Figure 2.1). Point mutation and deletion constructs were amplified using wild-type gene present in the *pHis*17 vector as a template (Table 2.1). PCR product was checked on EtBr stained agarose gel and purified using a Qiagen PCR purification kit. Purified DNA was used as a primer for RF PCR (Figure 2.1) (van den Ent and Löwe, 2006). The methylated parental plasmid was digested using DpnI enzyme for 3-4 hrs at 37 °C and transformed into NEB-Turbo electrocompetent cells. Colonies were screened for positive clones using restriction digestion. All clones were confirmed by sequencing.

Table 2.1 Primers used for cloning

S. No	Primer name	Sequence (5' → 3')
1	SG258 new R_p	GCTTTTAATGATGATGATGATGATGGGATCC GTTGCGCGCCAGGTGGGCGCGC
2	SG45 F_p	GTTTAACTTTAAGAAGGAGATATACATATGCG CGAAGGCGTCAAACTCC
3	MglB G61R F_p	GGCCTCGCTGACGGCCCGTAACGTGGCCGC GATGGG
4	MglB-SGAA-R F_p	CCACGTCACTGGCCCGGCTGACGGCCCGTA ACGTGCGCCGGATGGGTGGCCTGGCC
5	MglB SGA-R F_p	CCACGTCACTGGCCCGGCTGACGGCCCGTA ACGTGCGCGCGATGGGTGGCCTGGCC
6	MglB (Δ6) F_p	GTTTAACTTTAAGAAGGAGATATACATATGTA CGAAGAGGAGTTCACC
7	MglA D58A F_p	CCGCACGCTCTTCTTCGCCTTCCTGCCGCTG TCGC
8	MglA F56,57A F_p	CGGACCGCACGCTCGCCGCCGACTTCCTGC CGC
9	MglA Δ2 -8 F_p	GTTTAACTTTAAGAAGGAGATATACATATGCG CGAAATCAACTGCAAGATTG

Though all the planned constructs as given in the table were cloned successfully, and sequence confirmed through sequencing, the results section does not include the characterization of constructs 2, 4, 6 and 9.

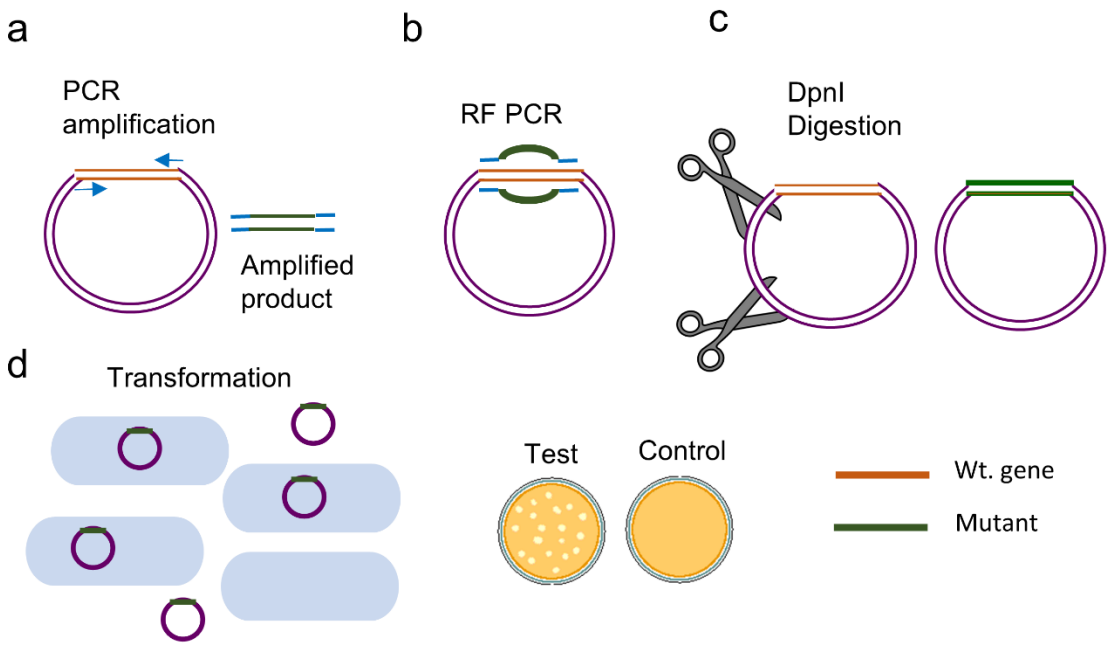

Figure 2.1. Steps involved in restriction free cloning

2.2 Protein expression

For overexpression, plasmid containing our gene was transformed in suitable *E. coli* expression strains. The cultures were grown at 37 °C and post-induction 18 °C for SofG and its mutants, while 30 °C for MglA, MglB, and their mutants. All cultures were grown in Luria broth (LB) media containing 100 µg/ml of ampicillin. MglB and SofG were transformed in BL21-AI and induced with 0.2% L-arabinose at OD_{600} value of 0.6, and 1.2 respectively. Similar protocol was followed for their mutants also. MglA was transformed in BL21(DE3) and 0.5 mM IPTG was used for induction at OD_{600} value of 0.8. To check expression, harvested cells were resuspended in lysis buffer (200 mM KCl, 50 mM Tris pH 8.0 and 10% glycerol) sonicated, pulse (1 second ON, 3 second OFF) at 60% amplitude for 1 minute. An aliquot of 10 µl was taken as total cell lysate, remaining sample was spun for 10 minutes at 21000 g to obtain a supernatant (soluble fraction of the lysate). 10 µl 2X SDS dye was added in total and soluble fractions and heated at 99 °C for 10 minutes then loaded on 12% SDS-PAGE gel (MglA and SofG) and 15% for MglB.

2.3 Protein Purification

2.3.1 Purification of SofG

6 L culture pellet was resuspended in 150 ml lysis buffer (200 mM KCl, 50 mM Tris pH 8.0 and 10% glycerol) and lysed using sonication for 6 minutes (1 second ON, 3 second OFF). Homogenized sample was then spun at 39000 g for 45 minutes at 4 °C. Supernatant was loaded on 5 ml Ni-NTA column (His Trap, GE Healthcare) pre-equilibrated with buffer $A200^{KCl}$ (200 mM KCl, 50 mM Tris pH 8). Hexa-histidine tag present in the C-terminus end of protein facilitated binding to Ni-NTA column. Bound protein was eluted using a step gradient of 5%,10%,20%,50% and 100% of buffer $B200^{KCl}$ (200 mM KCl, 50 mM Tris pH 8 and 500 mM Imidazole). Fractions containing purest eluted protein identified using SDS-PAGE gel analysis were dialyzed into Buffer $A25^{KCl}$ (25 mM KCl, 50 mM Tris pH 8) for 2 hrs. Dialysed protein was concentrated, flash frozen and stored in -80 °C. A similar protocol was followed for the SofG mutants, i.e., SofG Q140L. This protein was used for biochemical studies.

For crystallographic studies, we need higher concentration and homogenous protein. After Ni-NTA elution, 0.1 mM GDP was added to the fractions containing protein because an excess of GDP stabilized the protein. Protein was concentrated up to 500 µl and loaded onto size exclusion (Superdex 75 10/300, GE Healthcare) column equilibrated with $A25^{KCl}$ supplemented with 0.1 mM GDP and 2 mM $MgCl_2$. Fractions containing monomeric protein was concentrated, flash frozen and stored in -80 °C.

2.3.2 Purification of MglA

2 L culture pellet was resuspended in 60 ml lysis buffer (200 mM KCl, 50 mM Tris pH 8 and 10% glycerol) and lysed using sonication for 6 minutes (1 second ON, 3 second OFF). Homogenized sample was then spun at 39000 g for 45 minutes at 4°C. Supernatant was loaded onto a 5 ml Ni-NTA column (HisTrap, GE Healthcare) pre-equilibrated with buffer $A200^{KCl}$ (200 mM KCl, 50 mM Tris pH 8). Hexa-histidine tag present in the C-terminus end of protein facilitated binding to Ni-NTA column. Bound protein was eluted using step gradient of 5%,10%,20%,50% and 100% of buffer $B200^{KCl}$ (200 mM KCl, 50 mM Tris pH 8 and 500 mM Imidazole). Fractions containing purest eluted protein identified using SDS gel analysis were pooled and concentrated to less than 500 µl and loaded onto size exclusion (Superdex 75 10/300 GE) column

equilibrated with $A25^{KCl}$. Fractions containing monomeric protein was concentrated, flash frozen and stored in -80 °C. A similar protocol was followed for MglA mutants, i.e., MglA D58A, MglA Q82L, and MglA F56,57H.

2.3.3 Purification of MglB

MglB, MglBG61R, MglB SGAA-R, and $MglB^{Ct}$ (MglB with C-terminal 20 amino acids deleted) were purified using a similar protocol as described for MglA. For MglB construct without tag, MglB(ΔH6), ion exchange chromatography technique was used. Pelleted cells were resuspended in lysis buffer containing low salt lysis buffer $A50^{NaCl}$ (50 mM NaCl, 50 mM Tris pH 8 and 10% glycerol) and homogenized using sonication for 6 minutes (1 second ON, 3 second OFF). Homogenized sample was then spun at 39000 g for 45 minutes at 4 °C. The supernatant was loaded onto an ion exchange column QHP (GE Life Sciences). The column was pre-equilibrated with buffer $A50^{NaCl}$ (50 mM NaCl, 50 mM Tris pH 8.0). At pH 8.0, protein will become negatively charged anion since it is at a pH above its pI. This will facilitate binding of protein to the positively charged resin (anion exchange column). Bound protein was eluted using a linear gradient of 0 to 30% buffer $A1000^{NaCl}$ (1000 mM NaCl, 50 mM Tris pH 8). Fractions containing protein was dialyzed into buffer $A25^{NaCl}$ (25 mM NaCl, 50 mM Tris pH 8) for 2 hrs. Dialysed protein was filtered to remove aggregates of protein if present and loaded onto MonoQ 10/100 (GE Life Science) column using a 50 ml SuperLoop (GE Life Science). Bound protein was eluted using a linear gradient of 0 to 30% buffer $A1000^{NaCl}$ (1000 mM NaCl, 50 mM Tris pH 8). Fractions containing protein was concentrated and loaded onto size exclusion (Superdex 75 10/300 GE) column equilibrated with $A25^{KCl}$. Fractions containing dimeric protein was concentrated, flash frozen and stored in -80 °C.

2.3.4 Concentration estimation of purified proteins

Protein concentration was estimated by the Bradford method (Serra and Morgante, 1980). When Coomassie dye under acidic condition binds to basic amino acids of the protein, formation of protein-dye complex changes the color of reagent from brown to blue. Absorbance was measured at 595 nm, and the standard curve was plotted using known concentrations of BSA. Slope obtained from the standard curve was used for concentration estimation of protein (Figure 2.2).

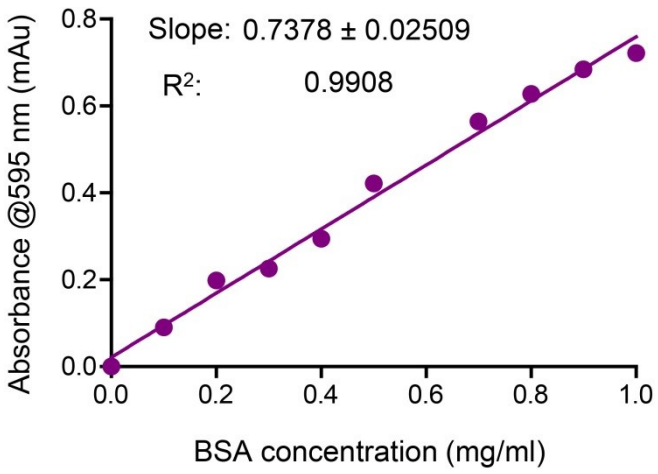

Figure 2.2. Bradford standard plot (one representative)

2.4 Size exclusion chromatography for protein-protein interaction

Size exclusion chromatography (SEC) separates protein molecules based on their size and shape. Proteins with higher size elute earlier and those with lower size elute later. SEC can be used for size estimation of globular proteins. We used this method to determine if SofG can form complex with MglB in the presence of different nucleotides (GDP or GTP/GMPPNP). Interaction of SofG and MglB will form a higher size protein complex. Higher size protein complex elutes before SofG. Superdex 75, 10/300 (GE Life Sciences) column was used for analysis, 0.5 ml fractions were collected and checked on the SDS-PAGE gel. For studies without nucleotide, column was pre-equilibrated with $A25^{KCl}$ and for studies with nucleotide column was pre-equilibrated with $A25^{+GTP}$ (25mM KCl, 50 mM Tris pH 8,0.1 mM GTP, 2mM $MgCl_2$) or $A25^{+GDP}$ (25 mM KCl, 50 mM Tris pH 8, 0.1 mM GDP, 2mM $MgCl_2$). 900 µl of a solution containing 18 µM SofG and 42 µM MglB (ratio of 1:2.5) protein in buffer $A25^{KCl}$ was injected with or without nucleotide (2 mM GTP or 2 mM GDP) and 2 mM $MgCl_2$.

2.5 Thermal shift assay

Thermal shift assay was used for checking protein stability and nucleotide binding (Senisterra et al., 2006). In a reaction volume of 25 µl containing 2 µM of protein in buffer $A25^{KCl}$, SYPRO Orange dye was added a final concentration of 5X. For nucleotide binding, buffer $A25^{+GTP}$ (25 mM KCl, 50 mM Tris pH 8, 0.1 mM GTP, 2 mM

$MgCl_2$) or $A25^{+GDP}$ (25 mM KCl, 50 mM Tris pH 8, 0.1 mM GDP, 2 mM $MgCl_2$) were used. After the reaction mix was prepared, these conditions were added to 96-well PCR plate and sealed with sealing tape. The plate was spun for 30 sec at 4000 rpm. Bio-Rad CFX96 real-time PCR machine was used to monitor the change in fluorescence of SYPRO Orange. The reaction was then heated from 4 °C to 90 °C with an increment of 0.4 °C for 70 minutes. As protein unfolds, the hydrophobic regions get exposed. SYPRO orange dye specifically binds to hydrophobic regions of the protein (Figure 2.3). Binding of the dye causes an increase in fluorescence, which is monitored and plotted using GraphPad Prism. T_m was estimated by plotting change in fluorescence with temperature (dF/dT) vs temperature.

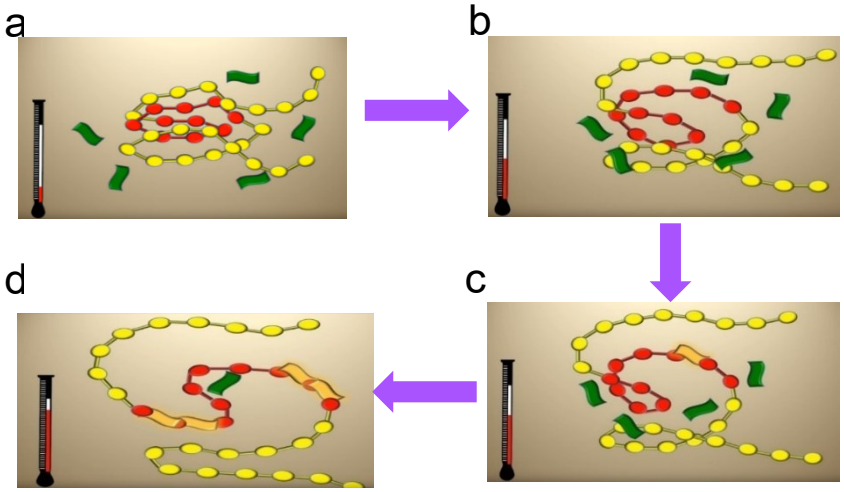

Figure 2.3. Thermal denaturation of protein

SYPRO orange dye (green) binds to hydrophobic regions of protein (red). Adapted from www.lifetechnologies.com/protein-thermal-shift

2.6 GTP hydrolysis assay

GTPase activity was measured using NADH coupled enzymatic assay (Kiianitsa et al., 2003). The GTP hydrolyzing enzyme converts GTP to GDP while pyruvate kinase uses PEP (phosphoenol pyruvate) and GDP to produce GTP and pyruvate. LDH (Lactate dehydrogenase) enzyme uses pyruvate and NADH to produce lactate and NAD^{+}. The decrease in NADH is directly proportional to the amount of GDP produced by the GTPase (Figure 2.4 A). The decrease in NADH absorbance was measured by monitoring absorbance at 340 nm using the multimode plate reader (Varioskan Flash, Thermo scientific). A master-mix was prepared in buffer $A25^{KCl}$ containing GTP (1

mM), NADH (600 µM), PEP (1 mM), $MgCl_2$ (5 mM) and PK/LDH enzyme mix (~25 U/ml). All the components were mixed in a 200 µl reaction volume and added in 96-well flat bottom plate. Proteins were added last to initiate the reaction. The concentrations of the GTPase used were 10 µM SofG or SofG mutants, 10 µM SofG or SofG mutants with MglB and its mutants (20 µM or 200 µM for 1:2 and 1:10 ratios respectively), 10 µM MglA or MglA mutants,10 µM MglA or MglA mutants with MglB and its mutants (20 µM or 200 µM for 1:2 and 1:10 ratios respectively).

Readings were taken at every 20 s for 2 hrs. NADH absorbance was converted to GDP produced using the conversion factor obtained from the standard curve (Figure 2.4 B, C). A standard curve was obtained by plotting different known concentrations of NADH (Figure 2.4B). Another standard curve was obtained by plotting different known concentrations of GDP (Figure 2.4C). Conversion factor obtained from both standard curves were similar. Data were plotted and analysed using GraphPad Prism.

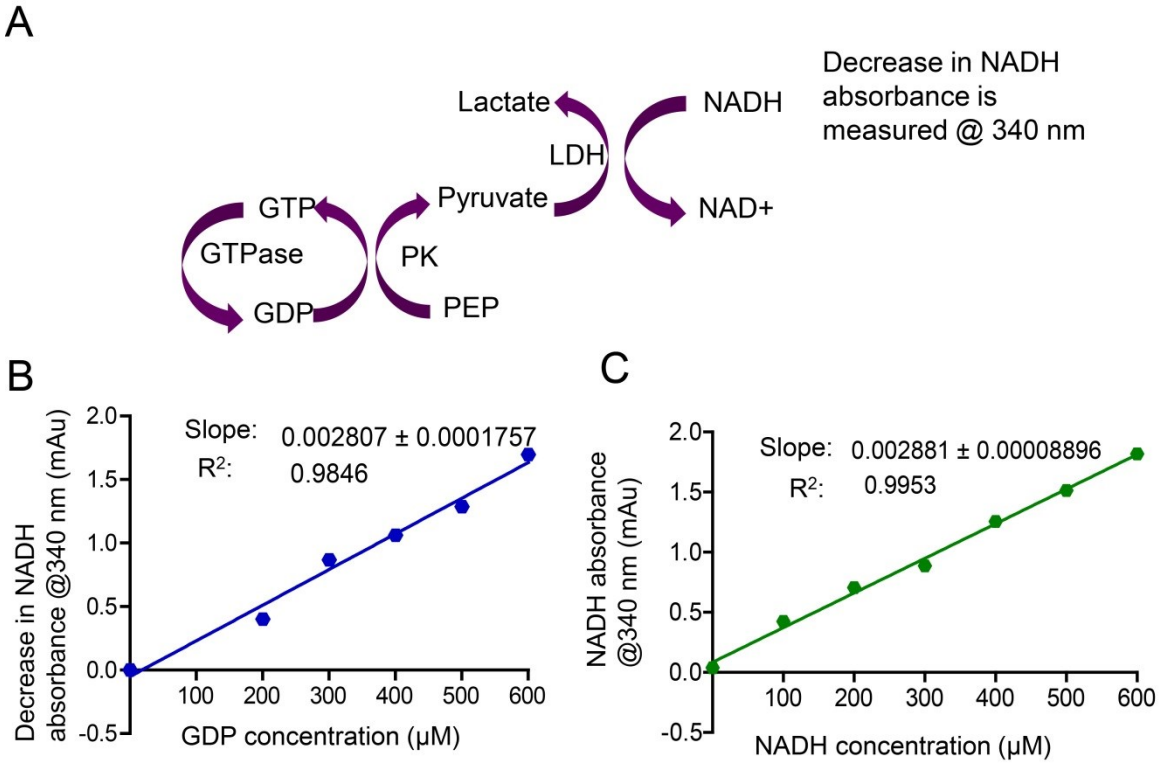

Figure 2.4. NADH coupled enzymatic Assay

A.Schematic representation of NADH coupled GTPase assay **B.** GDP standard plot (one representative) **C.** NADH standard plot (one representative)

2.7 Nucleotide binding assay using *mant*-GDP

Mant-GDP (fluorescent nucleotide analog) was purchased from Jena Bioscience. Emission spectra were taken between 390 nm to 490 nm after excitation at 360 nm to check the quality of *mant*-GDP. The intensity of *mant*-GDP was monitored at 440 nm after excitation at 360 nm. 400 nM *mant*-GDP was mixed with buffer $A25^{KCl}$ (25mM KCl, 50 mM Tris pH 8, 5 mM $MgCl_2$). 200 µl reaction mix was then added in the cuvette of path length 10*2 mm made of quartz (Hellma analytics). Experiments were performed in Fluoromax-4 (Horiba), with excitation and emission slit widths of 2 nm. Fluorescence intensity was monitored for 400 seconds. SofG (4 µM) was added in the cuvette at 400 seconds and mixed by pipetting. This was monitored till 1800 seconds. At 1800 seconds, 0.5 mM GDP was added, and fluorescence was monitored further for 1200 seconds (Figure 2.5A). Each value was divided by the average of the first 400 seconds readings. Data were plotted and analysed using GraphPad Prism.

2.8 Fluorescence anisotropy

Fluorescence anisotropy is widely used to obtain binding affinity of protein towards ligands or other proteins. To get binding affinity, MglA and MglB in the presence of different nucleotides (2 µM MglA and 100 nM *mant*-GDP or *mant*-GppNHp) was titrated against increasing concentrations of MglB. Binding of MglB to *mant*-nucleotide bound MglA increases anisotropy which was measured (Figure 2.5B). The excitation and emission were 360 nm and 440 nm. Experiments were performed in Fluoromax-4 (Horiba), with excitation and emission slit widths of 2 nm. 200 µl reaction mix was then added in the cuvette of path length 10*2 mm made of quartz (Hellma analytics). Initial value of *mant*-nucleotide bound MglA was subtracted from all the points (blank subtraction). GraphPad Prism was used for plotting anisotropy values against MglB concentration (in µM). Data were fitted using one-site specific (single binding site between MglA and MglB) equation ($Y=B_{max}*X/ (K_d + X)$ to obtain K_d value.

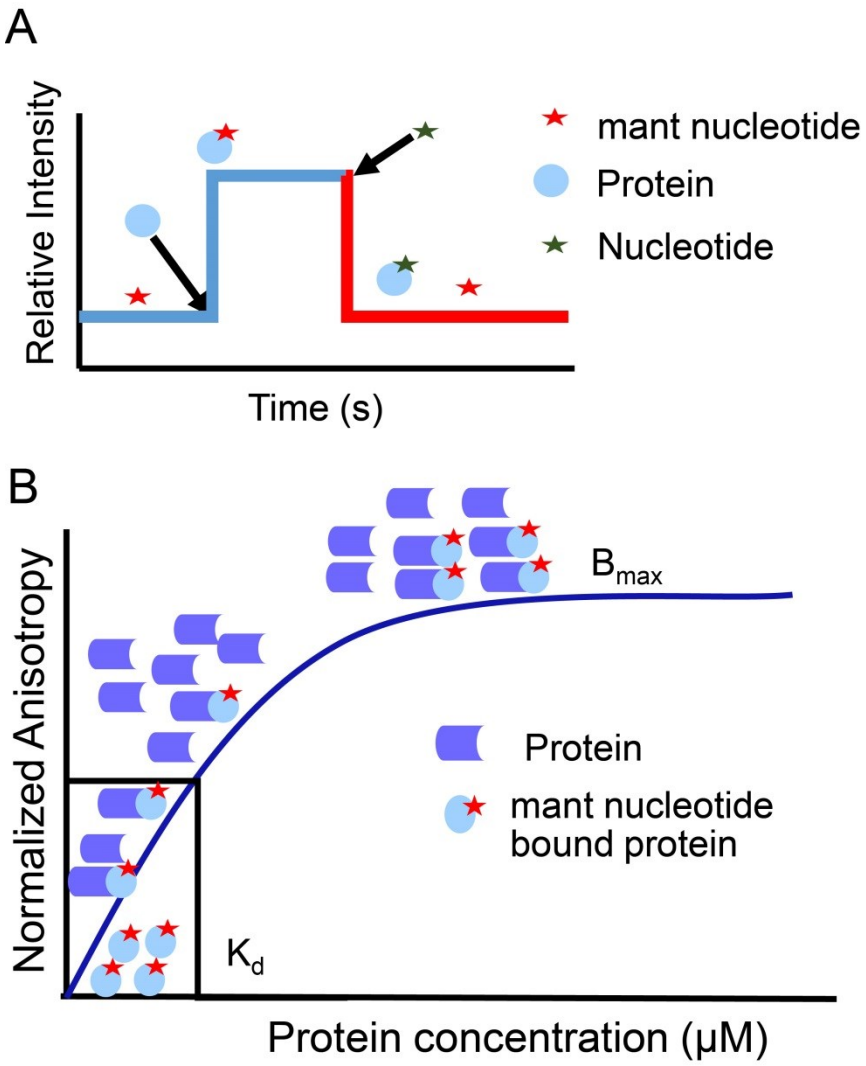

Figure 2.5 Fluorescence kinetics and anisotropy

A. Schematic representation of *mant* nucleotide association and dissociation on protein using fluorescence kinetics. **B.** Schematic representation of fluorescence anisotropy approach for monitoring protein-protein interaction

2.9 Sequence and structural analysis

Sequences were obtained from the list acquired from Wuichet et al., 2014, and downloaded from UniProtkb (Wuichet and Søgaard-Andersen, 2014). Individual lists for coupled and orphan sequences were generated manually. The presence of roadblock domain and small GTPase fold respectively for MglB and MglA was confirmed using SMART (Simple Modular Architecture Research Tool) analysis (Letunic et al., 2002). Sequences lacking this domain or fold were excluded from

further analysis. Sequences were analyzed using JalView (Clamp et al., 2004). MUSCLE algorithm was used to generate Multiple sequence alignment (MSA) (Edgar, 2004). MglB sequences were analysed to identify C-terminal extension. Extensions longer than 15 amino acids beyond roadblock fold were considered as C-terminal extension. MglA sequences corresponding to MglB C-terminal extension with negative charged were analysed for the presence of positively charged residues in α5 helix of MglA. Conservation-based logos were generated from sequence alignment using Skylign or Weblogo (Crooks et al., 2004; Wheeler et al., 2014). Structure were analysed using PyMol suite.

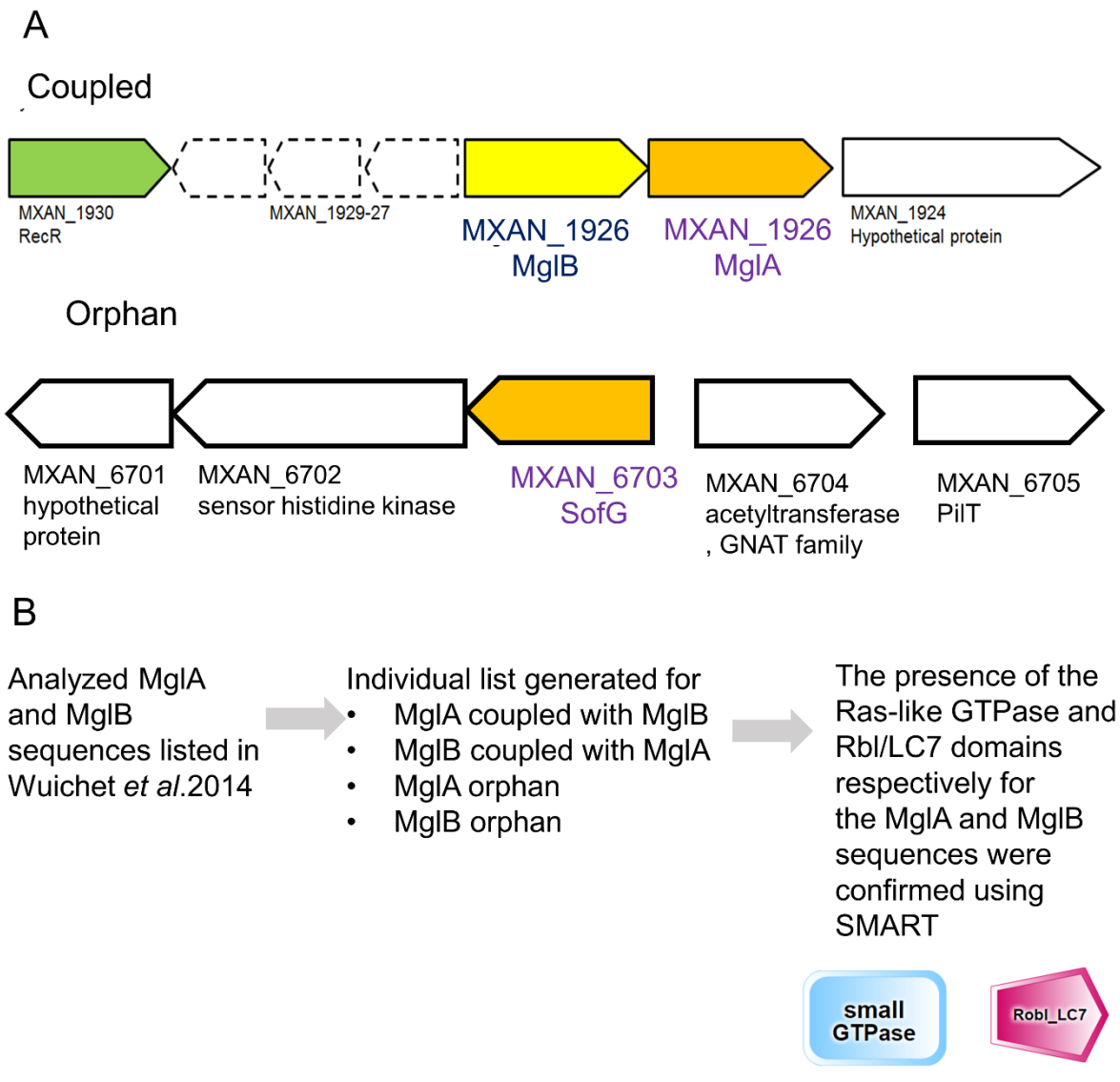

Figure 2.6. Sequence analysis

A. Coupled - MglA and MglB in the same operon. Orphan - only MglA or MglB in the operon **B.** Methodology of sequence analysis

Chapter 3. Results

Earlier work from lab resulted in the cloning of different constructs of SofG (Birjeet Singh, MS thesis, 2016; Sonal Lagad, MS thesis, 2017). Among all constructs, SofG construct with the N-terminal 60 amino acids deleted gave optimal expression and solubility which was further purified in the presence of excess of GDP. The yield obtained after purification was not sufficient for structural studies and extensive biochemical assays could not be performed as protein was purified in the presence of GDP. Earlier attempts to purify SofG without nucleotide were not successful. Purification of SofG needed further optimization.

3.1 Purification attempts of different constructs of SofG

Over-expression of remaining constructs (Figure 3.1 B) was checked in Bl21AI, Bl21(DE3), C41, and C43 strains of *E. coli*. To optimize expression, post induction, cultures were induced at different optical densities and incubated at various temperatures (37 °C, 30 °C and 18 °C). Protein expression and solubility were checked comparing samples prepared from induced and uninduced cells on SDS-PAGE gel. SG(60-277) construct showed good expression, but solubility was less (Figure 3.1A,B). SG, SG277, and SG18 showed less expression and solubility. Despite all expression optimization attempts, expression or solubility was less. During purification attempts from a 1-litre culture, SG, SG277 and SG (60-277) did not bind the Ni-NTA column (Figure 3.1C,E,F). SG18 had so many non-specific proteins bands which bound to the column and eluted (Figure 3.1D). All these purification attempts reconfirmed that SofG was the best construct for further characterization.

3.2 Purification optimization of SofG

SofG (UniProt MXAN_6703) consists of C-terminal and N-terminal extensions to the canonical G-domain (Figure 3.1 A). The C-terminal extension is 40 amino acids and forms two α helices (Figure 3.2 A). For N-terminal extension, no secondary structure was predicted.

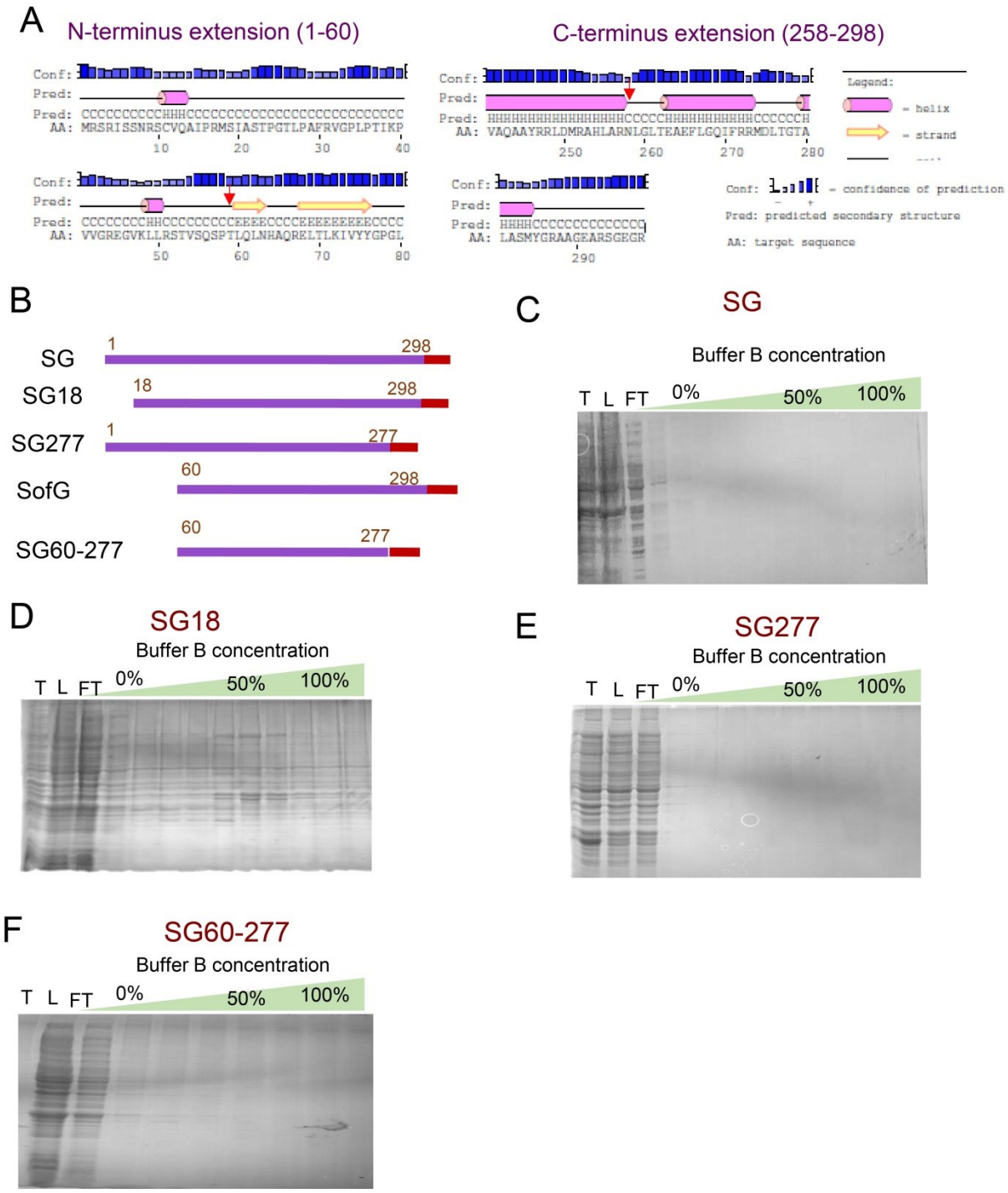

Figure 3.1- Purification attempts of different constructs of SofG

A. Secondary structure prediction (Psipred) for N and C-terminus extension of SofG. No significant secondary structure was predicted for first 60 amino acids **B.** Schematic representation of SofG constructs. Amino acids (violet), hexa-histidine tag (red) **C-F.** SDS PAGE gel representing Ni-NTA elution of different construct of SofG T-total, L-load, FT- flow through

SofG bound to Ni-NTA column and was present in reasonable amount in the eluted fractions. However, protein precipitated instantaneously and more than 95% of the protein was lost in the precipitate. To optimize purification after Ni-NTA, different purification strategies were tried.

i) *Ni-NTA elution followed by ion exchange chromatography*: After Ni-NTA elution, protein was dialyzed in buffer containing low salt and loaded onto ion exchange columns. Anion exchange and cation exchange columns were connected in series during loading and elution was performed individually for each column using increasing gradients of salt. SofG did not bind to anion exchange or cation exchange columns at pH 8 (Figure 3.2 B).

ii) *Ni-NTA followed by ammonium sulfate precipitation*: 50% of ammonium sulfate precipitated the protein, but pellet fraction obtained after centrifugation could not be resolubilized in buffer (Figure 3.2 C).

Since both these strategies were not optimal for purification, I proceeded with a purification involving Ni-NTA affinity chromatography followed by gel filtration. The final optimized protocol is discussed in detail in the materials and methods section (Chapter 2).

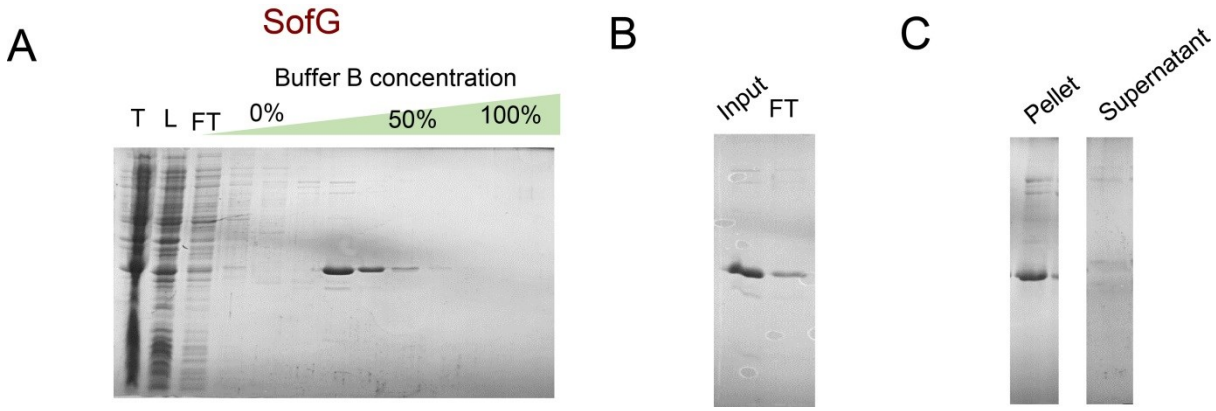

Figure 3.2 Purification optimization of SofG

A. SDS gel representing Ni-NTA elution of SofG T-total, L-load, FT- flow through. **B.** Anion exchange chromatography of SofG Input and FT. SofG did not bind to anion exchange **C.** Ammonium sulphate precipitation SofG is present in pellet and absent in supernatant

3.3 Characterization of SofG

3.3.1 Oligomeric status

To check the oligomeric state of SofG, size exclusion chromatography was performed. Purified protein was injected onto size exclusion column which separates molecules based on their size and shape. SofG eluted at volume 13 ml, which suggested that SofG is monomeric (Figure 3.3 B). Protein was mixed with GDP or GTP and injected onto size exclusion column to check if SofG forms higher order oligomers in the presence of nucleotide. SofG eluted at 13 ml in the presence of either GDP or GTP suggesting that SofG is monomeric in the presence of nucleotides too.

3.3.2 Protein stability measurements by thermal shift assays

Thermal shift assay indicated that SofG is well folded. T_m (melting temperature) of SofG was observed to be 38.2 ± 0.5 °C. Similar experiments were performed in the presence of GDP and GTP. T_m values for SofG in the presence of GDP and GTP were 50.4 ± 0.5 °C and 45.2 ± 0.4 °C respectively In the presence of GDP, T_m value was increased by 12 °C compared to the apo-protein while T_m value increased by 7 °C in the presence of GTP. Increase in T_m in the presence of nucleotide indicated that SofG bound to nucleotide (GDP or GTP) and the nucleotide-bound form is more stable than the apo (nucleotide-free) form. These observations suggested that SofG is most stable in the presence of GDP (Figure 3.3 C, Table 3.3).

3.3.3 Nucleotide binding

Thermal shift assay is an indirect method to check binding of ligands, and we will not be able to delineate between specific and non-specific binding of SofG to nucleotides. The fluorescence-based kinetic experiments were performed using *mant*-labeled nucleotides. Fluorescence intensity of *mant*-GDP was monitored before and after the addition of SofG. It was observed that addition of SofG increased fluorescence which suggested that SofG bound to *mant*-GDP. Now to check if the increase in fluorescence of mant-GDP was not due to non-specific sticking of the fluorophore, the labeled nucleotide was competed out with unlabeled GDP. This resulted in a decrease in fluorescence intensity (Figure 3.3 D). This experiment confirmed SofG binds to *mant*-GDP and binding is specific.

When a similar experiment was performed using *mant*-GppNHp, no significant fluorescence intensity increase was observed (Figure 3.3 E). *mant*-GppNHp binding was inconclusive as *mant*-GppNHp binding appeared unstable in comparison to *mant*-GDP and signal was less for *mant*-GppNHp. Further optimization is needed to get a good signal for *mant*-GppNHp binding. These assays confirmed that SofG was well folded and bound to the nucleotides.

3.3.4 GTP hydrolysis

GTP hydrolysis of SofG was qualitatively measured using NADH coupled enzymatic assay. GTPase activity of SofG was negligible like MglA. But in the presence of MglB, GTPase activity of MglA increased approximately by 35 folds (Figure 3.3 F). The absence of GTPase activity despite nucleotide binding prompted us to consider the requirement of an effector protein for SofG. To discover effector proteins that can interact and enhance the activity of SofG, the first candidate protein was MglB, which was the GAP for MglA. Hence, I performed sequence analysis of prokaryotic small Ras-GTPases and MglB-like sequences in the prokaryotic genome.

3.4 Sequence analysis of prokaryotic small Ras-like GTPases

Earlier sequence analysis showed that small Ras-like GTPases are widespread and present in all major bacterial phyla (Wuichet and Søgaard-Andersen, 2014). The analysis led to the discovery of two distinct families of prokaryotic small Ras-like GTPases MglA and Rup. MglA family was divided into five groups based on phylogenetic analysis. MglA-like proteins associated with the gene encoding an MglB-like protein in the same operon are called coupled while those without an associated MglB gene are called orphans (Figure 2.6 B). We analyzed the sequences of MglA and MglB, as present in the list in Wuichet et al., 2014. In 562 MglB sequences, 343 are coupled, and 219 were orphan. Among 391 MglA sequences, 340 are coupled, and 51 are orphan. The mismatch in the coupled sequences was observed due to the presence of multiple MglB sequences coupled to the same MglA or vice versa. Recent studies on MglB orphan (MglC) and MglA orphan (SofG) suggested that both MglA and MglB orphan genes are functional (Bulyha et al., 2013; McLoon et al., 2016).

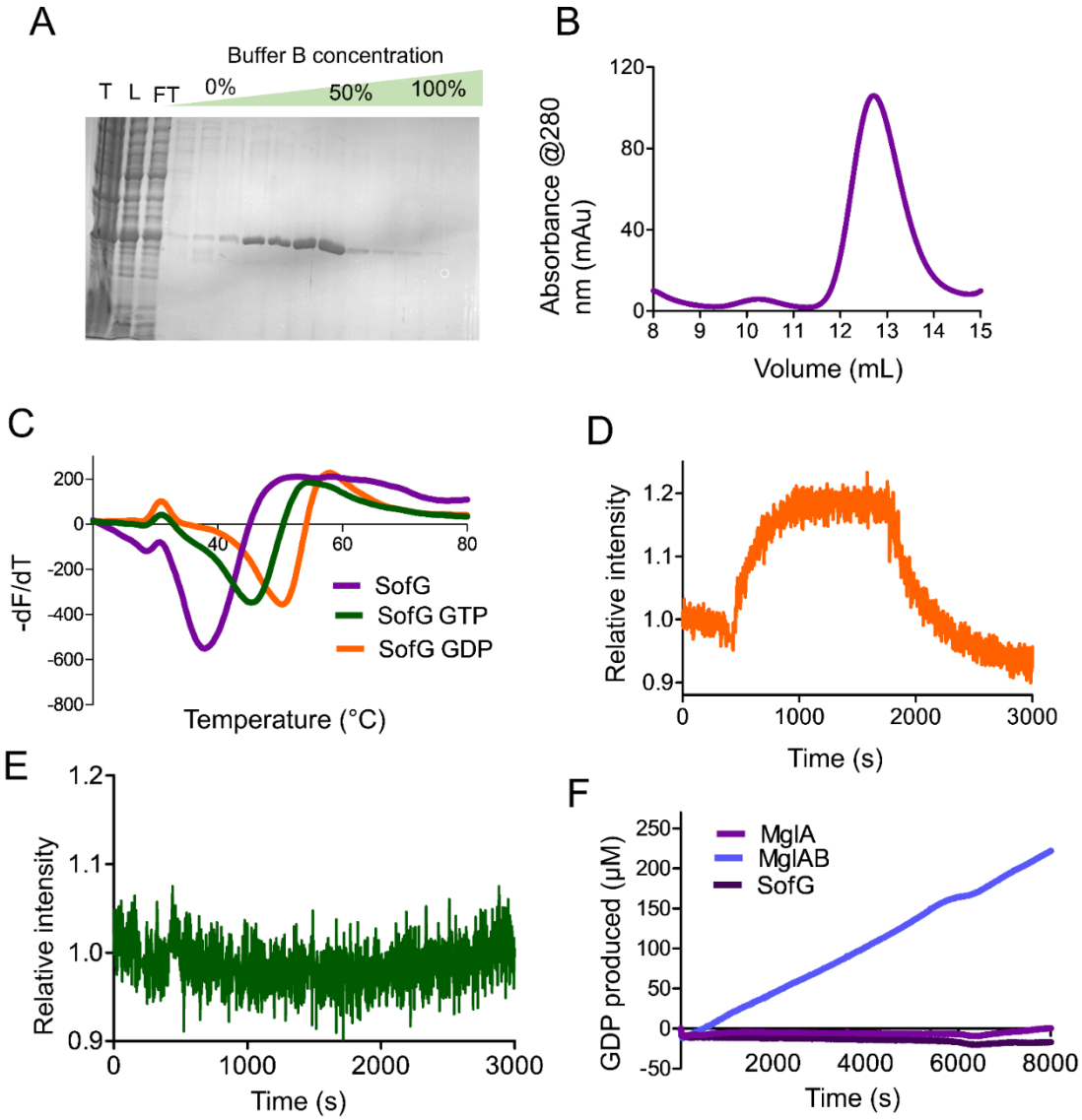

Figure 3.3 characterization of SofG

A. Ni-NTA elution profile of SofG using final optimized protocol T-total, L-load, FT- flow through **B.** Size exclusion chromatography profile of SofG using Superdex 75 column. SofG elutes at 13 ml and is homogenous. **C.** Thermal shift assay demonstrated SofG (violet; n=6, N=2) is folded. T_m increase in presence of GDP (orange; n=6 N=2) and GTP (green; n=6, N=2) suggest SofG binds to GDP and GTP **D.** *mant*-GDP binding to SofG increased fluorescence intensity and addition of unlabeled nucleotide decreased it, suggesting that SofG binds to GDP specifically (n=5, N=2). **E.** *mant*-GppNHp binding to SofG. No significant increase observed after SofG addition (n=2, N=1) **F.** GTPase activity of SofG (violet; n=8, N=4) is insignificant like MglA (blue; n=4, N=2). MglAB (dotted blue; n=8, N=2)

Note: From now N denotes number protein batches used and n denotes number of repeats.

3.4.1 Coevolution of MglAB interface

Since structural information on MglAB interaction is available for *Thermus thermophilus* and *Myxococcus xanthus*, we performed sequence analysis for co-evolution of interacting residues in MglA and MglB. MglA β2 strand flips to form the interaction interface with MglB (Miertzschke et al., 2011). Conservation of β2 strand was checked in MglA coupled sequences. Interestingly, we found that β2 strand residues were conserved and two distinct residue conservation patterns were observed. One group had LFFDF motif in the β2 strand, while the other had VAMDF motif. Among 340 MglA coupled sequences, 56 sequences had LFFDF (later referred as MglA class 1) and the remaining had VAMDF motif (later referred as MglA class 2). The 56 sequences with LFFDF motif belonged to group 1 of MglA family, while the rest with VAMDF motif includes groups 2 -5, according to classification by Wuichet et al., 2014.

We further checked the conservation of α2 helix of MglB (important for MglB dimerization and interaction with MglA). Conserved residues were different in the respective MglB sequences coupled to each MglA class, consistent with the different sequence motifs of the corresponding MglA sequences (LFFDF and VAMDF). MglA F56 and F57 interact with G61, which was conserved in corresponding MglB sequences. The sequence conservation of interacting residues of the motif are shown in (Figure 3.4 C). As no structural information is available for MglA group 2 members, we checked if VAMDF motif could potentially interact with its respective MglBs. Interestingly we found a conserved leucine, which can potentially interact with A56 of MglA. The F → A interacting pair (MglA F56 to MglB A68) in class 1 is substituted by A → L interacting pair (,MglA A56 to MglB L68) in class 2. The replacement with a smaller residue (F to A) is accompanied by a corresponding change to a bigger residue (A to L) in MglB (Figure 3.4 D, E). Based on these analyses, we hypothesized that MglA class 2 members can also potentially interact with their corresponding MglB.

Next, we checked if a MglA orphan can potentially interact with a coupled MglB in the same organism. As SofG is a MglA class 1 orphan and LFFDF motif is present, we limited our analysis to MglA class 1 orphan. First, we checked the presence of MglB like protein coupled with MglA in the same organism. Interestingly we found out of 26 MglA orphan sequences, 23 sequences had MglB sequences associated with coupled MglAs in the same organism and MglB α2 helix had a conservation pattern similar to

MglB corresponding to class 1 MglA. Based on these observations, we hypothesized that MglA orphans could potentially interact with MglB present in the same organism.

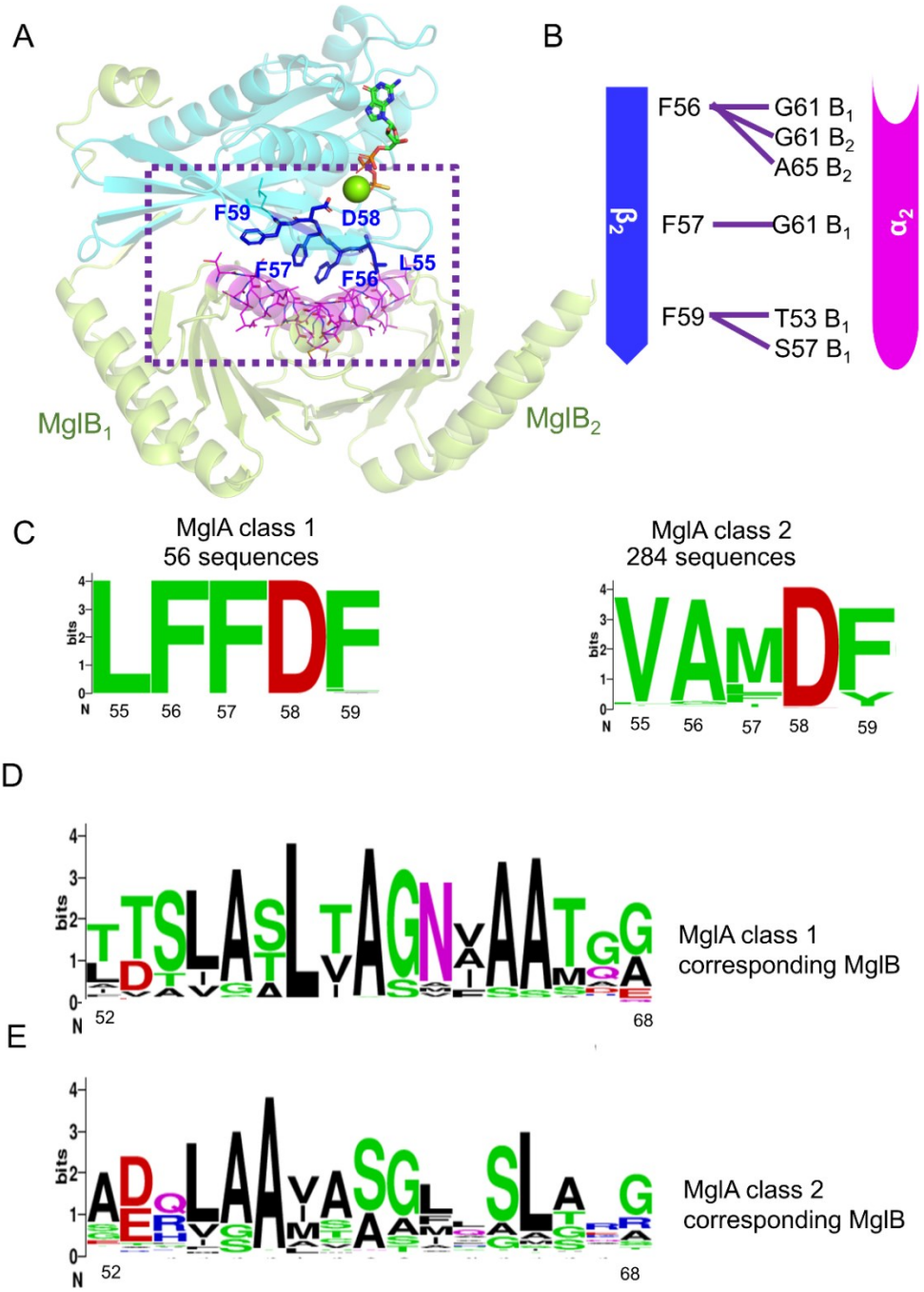

Figure 3.4 Sequence analysis of MglA and MglB proteins

A. *Myxococcus xanthus* MglAB Interface. MglA β2 strand (blue-residue shown in sticks). α2 helix of MglB (magenta residues shown in line representation) **B.** Interaction map between MglA phenylalanines (56, 57 and 59) and MglB **C.** Conservation of MglA β2 strand residues **D.** Conservation of MglB α2 helix corresponding to MglA class 1 **E.** Conservation of MglB α2 helix corresponding to MglA class 2

3.4.2 Catalytic motifs

Next, we proceeded to compare the catalytic motifs of the two classes of MglA family identified based on coevolution of the MglB interacting residues. The small Ras-like GTPase family utilizes five conserved G motifs to carry out nucleotide binding and GTP hydrolysis (discussed in Chapter 1). Four of the G motifs (G1 – G4) involved in GTP binding and hydrolysis were analyzed in MglA sequences. The catalytic motifs also showed a characteristic signature, unique for each of the classes. G4 motif was conserved in MglA class 1 while in MglA class 2 it diverges from the classical NK[x]D motif. Lysine, which interacts with guanine base, was absent; instead, we observed a strong conservation of phenylalanine here (Figure 3.5). CVD9 is a MglA class 2 member which has GTPase activity (Wuichet and Søgaard-Andersen, 2014), suggesting that the deviant G4 motif of MglA class 2 indeed bound to the nucleotide. In the *Myxococcus xanthus* MglA structure, lysine formed a stacking interaction with the guanine ring. We hypothesize that the role of the conserved lysine could be taken by phenylalanine in this scenario.

Structural and biochemical studies have been carried out on *Myxococcus xanthus* and *Thermus thermophilus* MglA, both of which belong to MglA class 1., MglB drives the conformation change which helps arginine in G2 motif to attain optimal orientation for active hydrolysis (Miertzschke et al., 2011). This arginine residue was conserved in G2 motif of MglA class 1 preceded by a conserved threonine. In contrast to MglA class 1, arginine was absent in MglA class 2. Hence, the catalytic residue corresponding to arginine for GTP hydrolysis in class 2 GTPases is unidentified. G3 motif of MglA family differs from eukaryotic Ras superfamily (DxxGQ). MglA class 1 members possess TVPGQ and MglA class 2 members have GTPGQ (Figure 3.5).

3.4.3 Identification of a novel catalytically important residue

In prokaryotic small Ras-like GTPases, the most notable deviation from eukaryotic conserved motifs is the lack of aspartate (Walker B aspartate) in G3 motif, which is essential for coordination of water molecules and threonine side chain that are coordinated to Mg^{2+} (Figure 3.6 D). A superposition of the eukaryotic small Ras-like GTPase with MglA (Figure 3.6 A) structure showed that the D of LFFDF motif in MglA performs the same function as the D from G3 motif of Ras (Goitre et al., 2014;

Wennerberg et al., 2005) (Figure 3.6 C,D).This explained the presence of a conserved aspartate in all 5 groups of MglA family. Walker B aspartate is present in β3 strand in eukaryotic small Ras-like GTPases. In MglA walker B aspartate is present in β2 strand (Figure 3.6 A, B). This new novel motif is present in prokaryotic small Ras-like GTPases only.

In summary, the key findings of the sequence analysis include:

i) identification of a novel sequence motif in prokaryotic Ras-like GTPases, relevant for MglB interaction

ii) the aspartate corresponding to G3 motif of eukaryotic Ras-like GTPases is present in the newly identified motif

iii) MglB can potentially act as a GAP for SofG too.

In order to experimentally validate the key findings, we performed the experiments as described in the next section.

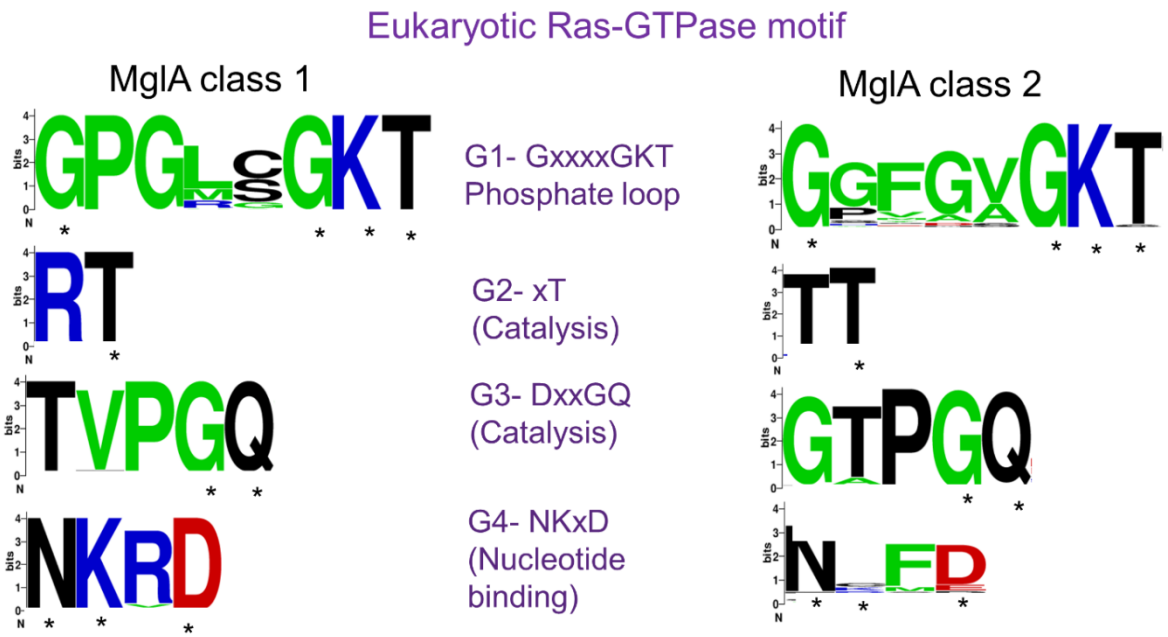

Figure 3.5 conservation of G-motif in different MglA classes

3.5 Biochemical characterization of MglA active site mutants

To find out the relevance of the conserved aspartate in prokaryotic GTPase, we proceeded with the biochemical characterization of constructs with point mutations of MglA, the prototypic GTPase of the prokaryotic family. Biochemical characterization of MglAQ82L (later referred as MglA^{Q}) – a residue with demonstrated catalytic role in

Thermus thermophilus MglA (chapter 1); and MglAD58A (later referred as MglA^{D}) – aspartate present in the LFFDF motif; were performed.

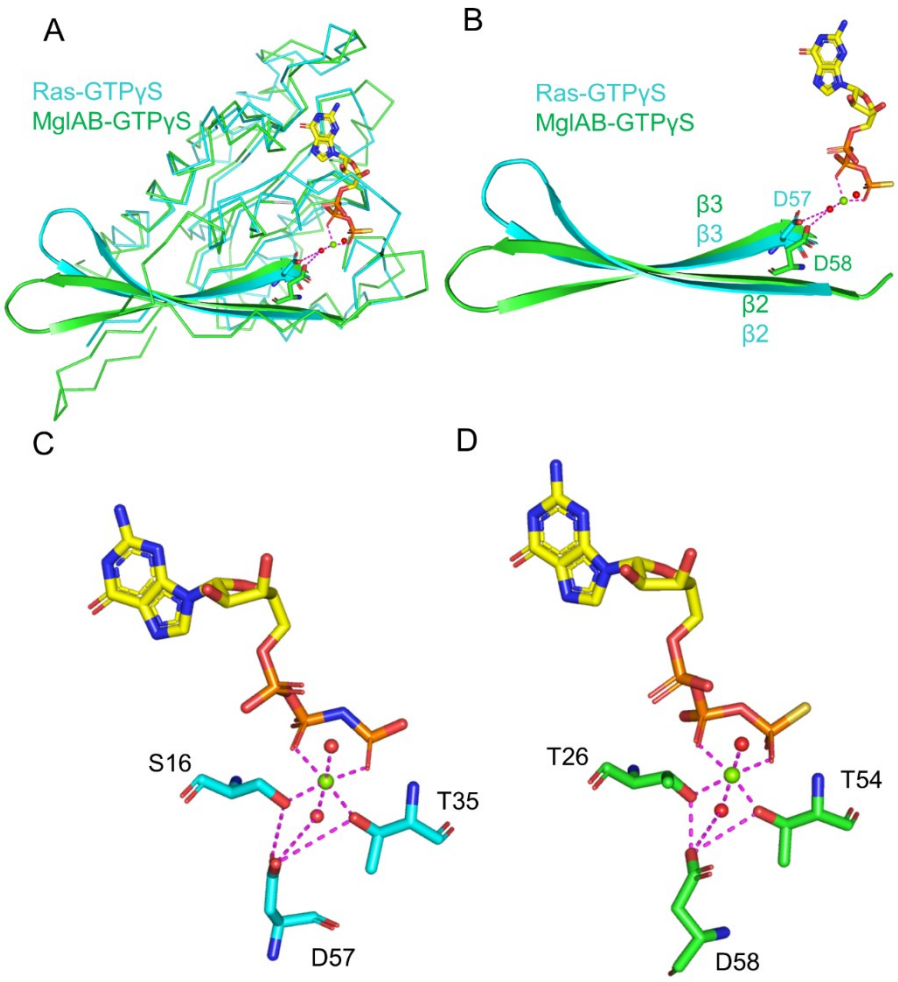

Figure 3.6 Walker B aspartate coordinates water and threonine which coordinates Mg^{2+}

A. Comparison between MglAB-GTPγS (green) and Ras-GTPγS (5P21) (cyan) both shown in ribbon representation. β2 and β3 strands are shown in cartoon **B.** In Ras Walker B aspartate is present in β3 strand, while in MglA it is present in β2. **C.** Mg^{2+} co-ordination in Ras **D.** Mg^{2+} co-ordination in MglA.

The mutants were purified by Ni-NTA (affinity chromatography) followed by size exclusion chromatography. Both mutants eluted at 13.5 ml in Superdex 75 (size exclusion column); this indicates both mutants are monomeric and pure (Figure 3.7 A, B, C). As I mentioned earlier, MglB is a GTPase activating protein of MglA (Zhang et al., 2010). NADH coupled GTP hydrolysis assay was performed in the presence and

absence of MglB. MglA has insignificant GTPase activity. In the presence of MglB, activity increased by several fold. $MglA^{Q}$ and $MglA^{D}$ mutants showed very low GTPase activity even in the presence of MglB. MglB addition did not enhance the GTPase activity of $MglA^{D}$ and $MglA^{Q}$ (Figure 3.7 E).

Since there was no activity observed in the mutants, we checked if these mutants are unfolded or deficient in nucleotide binding. Thermal shift assay was performed to get information about the folded state of these mutants. $MglA^{Q}$ and $MglA^{D}$ were well folded, and the unfolding temperature was like MglA. To confirm GDP and GTP binding of these mutants, thermal shift assay was performed in the presence of GDP and GTP. In the presence of GDP and GTP, T_m values increased approximately 10°C and 12°C for GTP and GDP respectively. Similar T_m increase was observed for MglA, which indicates that GDP and GTP binding of this mutants is not affected (Figure 3.7 D) (Table 3.1). MglB binding affinity of $MglA^{Q}$ is not affected (Figure 3.7F) (Table 3.1). Above experiments confirmed that the mutation of D58 and Q82 affected GTP hydrolysis.

Table 3.1. T_m value of MglA and its mutants

Protein / Condition	MglA (°C)	$MglA^{D}$ (°C)	$MglA^{Q}$ (°C)
No-nucleotide	49.9 ± 0.2	48.9 ± 0.3	49.8 ± 0.3
GDP	60.4 ± 0.1	61.5 ± 0.2	61.4 ± 0.2
GTP	57.9 ± 0.1	58.7 ± 0.1	57.8 ± 0.1

Table 3.2. K_d estimates for MglB binding

Protein	m-GDP (μM)	m-GppNHp (μM)
MglA	0.22 $\pm$ 0.13	0.21 $\pm$ 0.08
$MglA^{Q}$	0.20 $\pm$ 0.05	0.29 $\pm$ 0.05

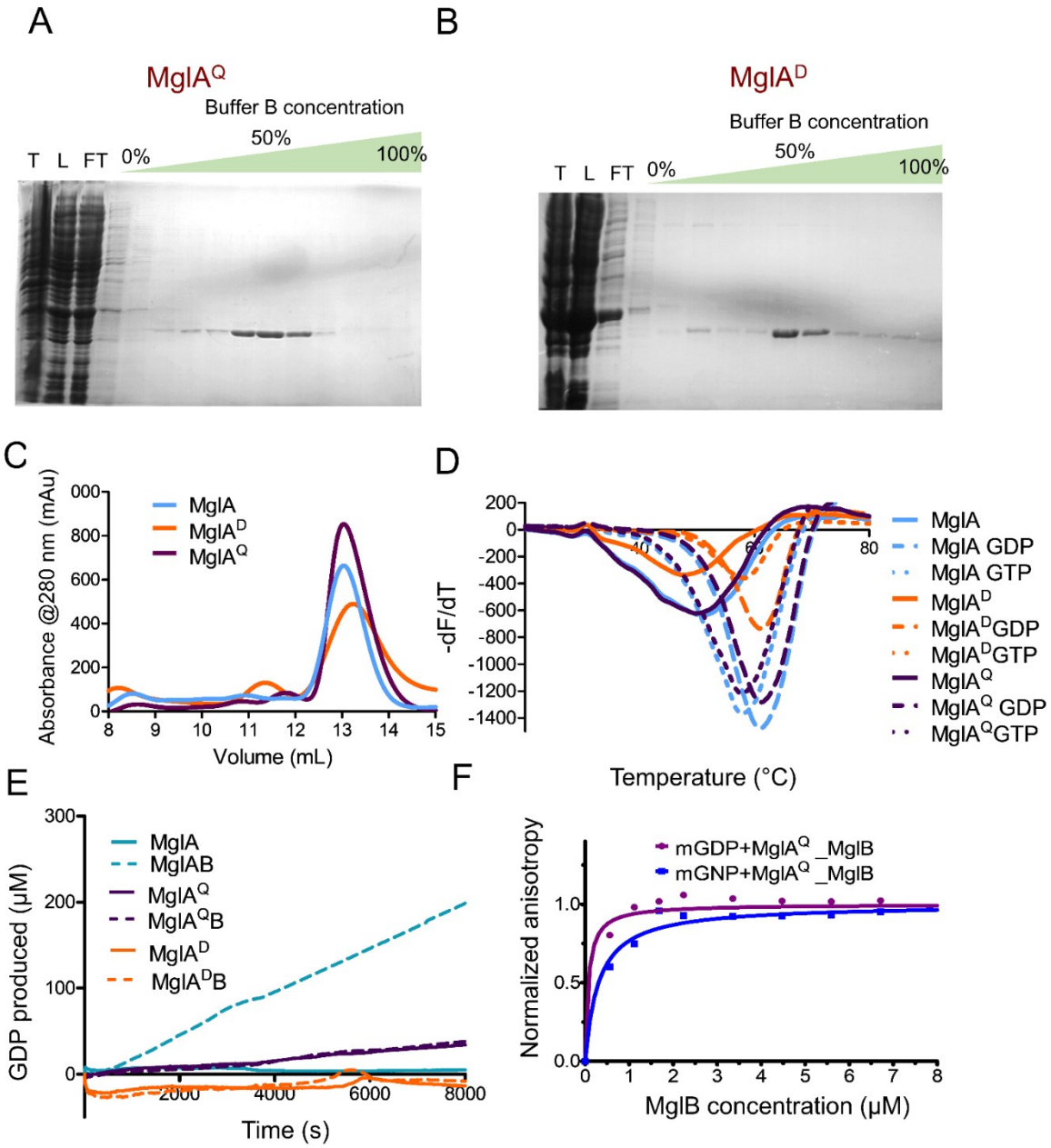

Figure 3.7 Biochemical characterization of MglA mutants

A-B. Ni-NTA elution profile of $MglA^Q$ (A) and $MglA^D$ (B) **C** Size exclusion chromatography elution profiles of MglA (blue), $MglA^Q$ (violet) and $MglA^D$ (orange) indicate both mutants are monomeric. **D**. Stability of mutants. T_m shift in presence of nucleotide is suggestive of binding. MglA (blue; n=9, N=2), $MglA^Q$ (violet; n=6, N=2) and $MglA^D$ (orange; n=3, N=1). Dashed and dotted lines represent GDP and GTP binding, respectively. **E.** GTPase activity of MglA (blue; n=12; N=3), $MglA^Q$ (violet; n=6, N=4) and $MglA^D$ (orange; n=2, N=1). Presence of MglB is represented with

dashed line. MglA^{Q} and MglA^{D} are GTPase deficient. **F.** Fluorescence anisotropy measurement for MglB titrated against mGDP bound (purple n=4) and m-GppNHp bound (blue n=4) MglA^{Q}. Binding affinities towards MglB were not affected.

3.6 Characterization of interface mutants of MglA and MglB

Sequence and structural analysis suggested β2 strand of MglA and α2 helix of MglB formed the major interface region; interestingly these residues are conserved across MglA- and MglB-like proteins in other organisms. Mutations in MglA β2 strand phenylalanine (F57, F59) to histidine made the protein unstable, and higher precipitation was observed during purification. Sufficient protein yield was not obtained for activity studies (data not shown). MglB G61, a conserved residue of MglB interface, was mutated to arginine (later referred as MglB$^{G)}$. MglB^{G} was purified using the protocol discussed in materials and methods. First, we checked the oligomeric status of MglB^{G} using size exclusion chromatography (Superdex 75). MglB^{G} formed a dimer like MglB, which suggested that MglB^{G} is stable and dimeric interface was not affected after mutation (Figure 3.8 A). Next, we checked the effect of MglB^{G} in GTP hydrolysis of MglA. GTPase activity of MglA in the presence of MglB^{G} was done in two different ratios 1:2 and 1:10. In the presence of MglB^{G} GTPase activity was reduced by several fold. Higher ratio of 1:10 did not also catch up to MglB (1:2) (Figure 3.8 B). These results revealed that MglB^{G} affected MglA GTPase activity by at least ten fold.

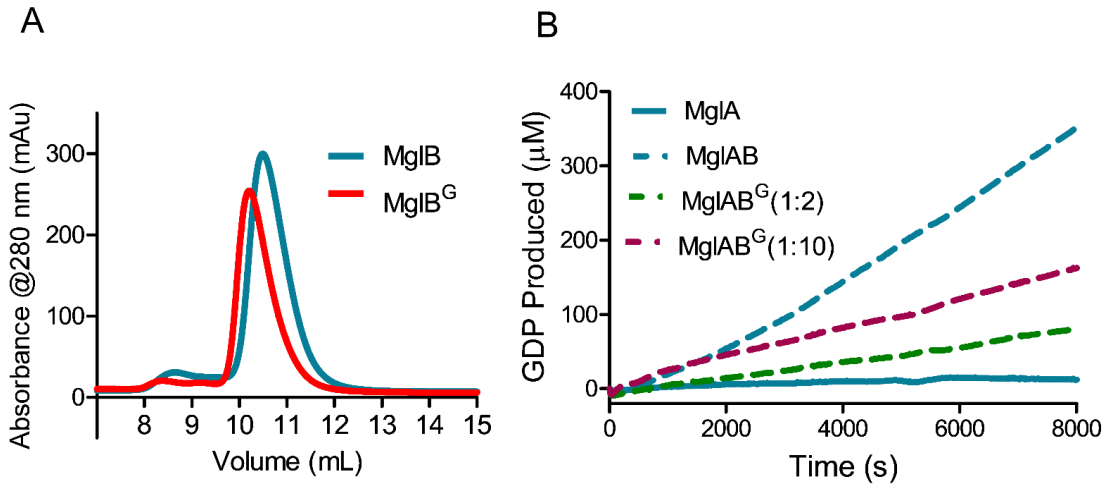

Figure 3.8. Reduction in GTPase activity in MglB^{G}

A. MglB^{G} forms dimer like MglB. Size exclusion chromatography of MglB (skyblue) and MglB^{G}(red) **B.** GTPase activity of MglA in presence of MglB^{G} is affected. MglA (sky blue) is shown in solid line with MglB presented in dotted line. MglA with MglB^{G} (1:2) (dashed green; n=8, N=1); MglA with MglB^{G} (1:10) (dashed purple n=4, N=1).[36]

3.7 MglB is a GAP for SofG

Sequence analysis suggested that MglB can interact with MglA orphans. SofG is a MglA orphan; this prompted us to check if MglB can act as GAP for SofG or not. We checked the GTPase activity of SofG in the presence of MglB. We found that GTPase activity of SofG was increased in the presence of MglB. To ensure this is not an experimental artifact, SofG active site mutant Q140L (later referred as $SofG^{Q}$) was purified. GTPase activity was checked for $SofG^{Q}$ in the presence of MglB. MglB did not enhance GTPase activity of $SofG^{Q}$. We further checked the folding state of $SofG^{Q}$ by thermal shift assay. The unfolding temperature of $SofG^{Q}$ was comparable to SofG. $SofG^{Q}$ bound to GDP and GTP, as a T_m shift was similar to SofG was observed. This suggested that nucleotide binding is not affected after mutation (Figure 3.9 B). Next, we checked the activity of SofG with the interface mutant $MglB^{G}$. GTPase activity of SofG in the presence of $MglB^{G}$ was reduced as compared to MglB (Figure 3.9 A). All these results indicated that MglB acts as a GAP for SofG, and the mechanism of GAP activity by MglB is common for both MglA and SofG.

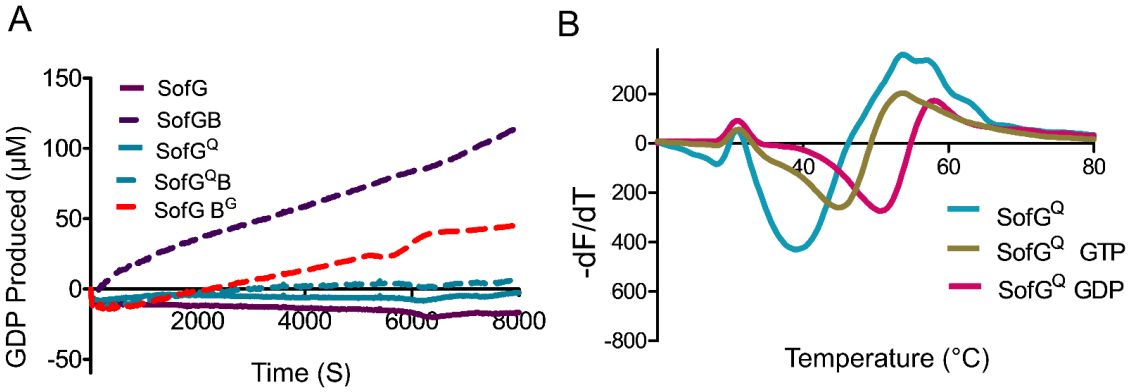

Figure 3.9 Characterization of SofG mutants

A. MglB enhances GTPase activity of SofG. SofG alone - solid line (violet; n=5, N=4); SofG with MglB dashed line (n=8 N=4); $SofG^{Q}$ active site mutant solid line (sky blue n=4, N=1); SofG with MglB dashed line (n=4, N=1). SofG with $MglB^{G}$ dashed line (red, n=3; N=1) **B.** Thermal shift assay of $SofG^{Q}$ (blue) in the presence of GDP (brown) and GTP (magenta). Increase in T_m value indicates binding to GDP and GTP (n=6; N=1)

Table 3.3. T_m values of SofG and SofG^Q

Protein / Condition	SofG (°C)	SofG^Q (°C)
No-nucleotide	38.2 ± 0.5	37.8 ± 0.8
GDP	45.2 ± 0.4	45.1 ± 0.6
GTP	50.4 ± 0.5	50.1 ± 0.3

3. 8 Interaction studies of SofG and MglB

Following observation of GTPase activation of SofG by MglB, binding of SofG and MglB was checked by size exclusion chromatography and Microscale thermophoresis (MST). In size exclusion chromatography, MglB and SofG elute at different elution volumes. SofG and MglB complex also elutes at same elution volume as MglB alone. In this experiment, SofG and MglB complex reaction mixture was prepared in buffer with and without nucleotides and injected in the size exclusion column (Superdex 75). If SofG-MglB complex is formed SofG will elute earlier (size of the complex is higher) which can be only checked by loading fractions on SDS PAGE gel to determine the presence of SofG in them. SofG bound to MglB only in the presence of GTP. Binding to MglB was not observed in the presence of GDP and without nucleotide.

Earlier work from lab showed that MglB interacted with MglA in the presence of GTP and GDP, while a C-terminal truncated construct of MglB (MglB^{Ct}) interacted with MglA only in the presence of GTP. Hence, the Ct-helix of MglB was proposed to be important for interaction in the presence of GDP and facilitated GDP to GTP exchange of MglA. Thus, Ct-helix contributes to GEF activity of MglB. SofG interaction with MglB is similar to MglB^{Ct} and MglA as it interacts only in the presence of GTP. Hence, we proceeded to carry out sequence analysis of Ct-helix of MglB sequences and their co-evolution with the MglA interacting interface.

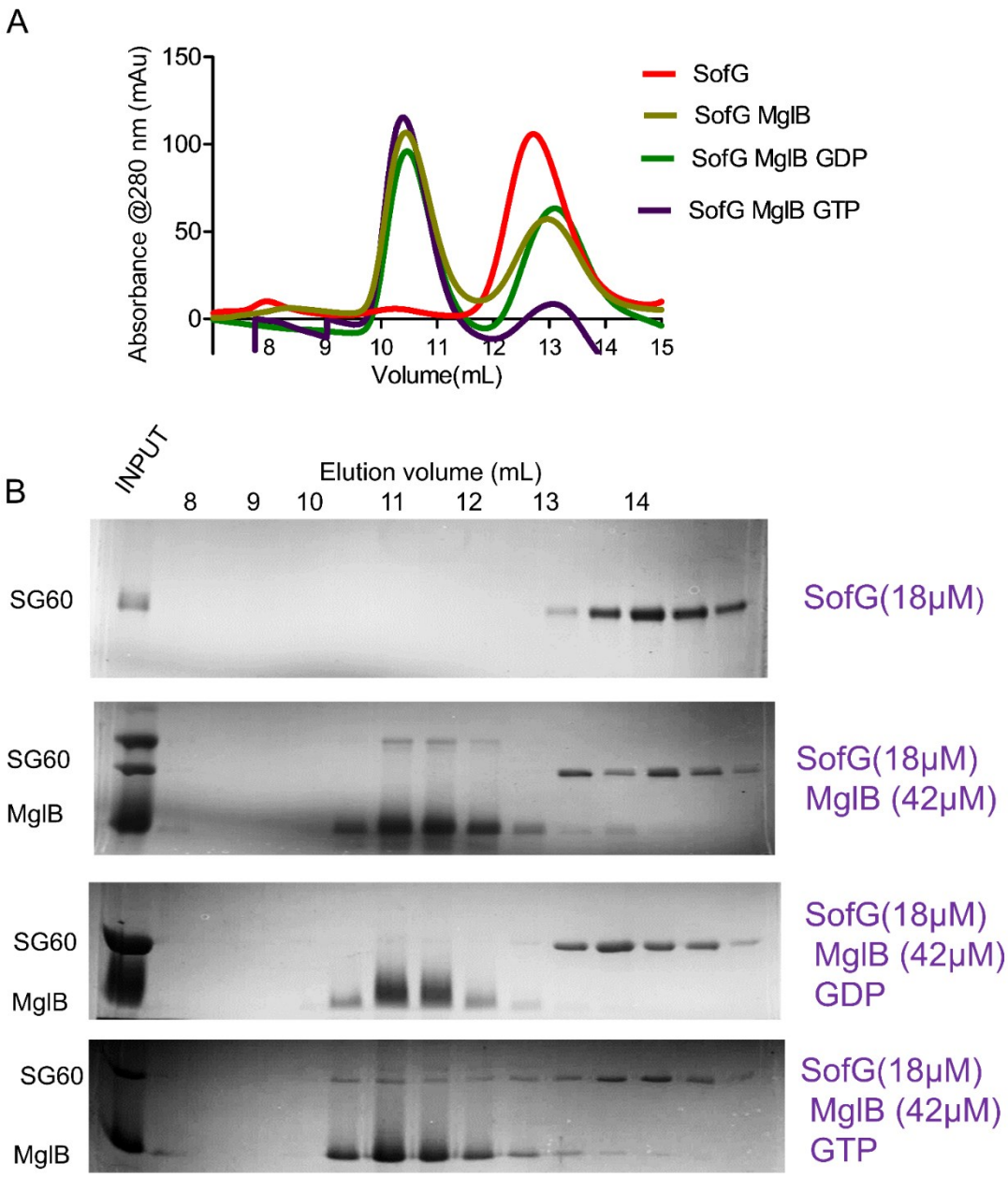

Figure 3.10. SofG interacts with MglB in presence of GTP, and not in the presence of GDP.

A. Size exclusion chromatography profile. SofG (red), SofG with MglB (light brown), SofG-GDP with MglB (green) and SofG-GTP with MglB (violet)

B. SDS PAGE gel for respective size exclusion chromatography profiles as explained in A.

MglB sequences were analyzed to find the presence of C-terminal extension (Ct) in those sequences. More than 15 amino acids beyond roadblock/LC7 fold were considered as Ct extension. We found that out of 343 coupled sequences, 66 had Ct

extension, and among 219 orphan sequences, 25 sequences had Ct extension. In *Mx* MglAB complex structure, MglB Ct extension forms a helix, which interacts with the α5 helix of MglA (Figure 1.5 A). Negatively charged amino acids (D150, D151, D152, and D153) of MglB Ct extension interact with positively charged amino acids in MglA (K181, K185) (Baranwal et al., unpublished).

Hence, we checked for the secondary structure of Ct extension and presence of 2-4 negative charged amino acids (aspartate and glutamate). Interestingly, we found out of 66 coupled sequences, 56 sequences showed a predicted helical region and the presence of negatively charged amino acid stretch (aspartate or glutamate) (Figure 3.11 A). Remaining MglB coupled (10 sequences) and MglB orphan (25 sequences) sequences showed a proline-rich region with no predicted secondary structure (Figure 3.11 C). Out of the 56 MglA sequences corresponding to MglB sequences with Ct extension with negatively charged amino acid stretch, 48 MglA sequences had positively charged amino acids (lysine or arginine) in the α5 helix (Figure 3.11 B). These positively charged amino acids were not conserved in remaining MglA sequences (Figure 3.11 D). This suggested MglA α5 helix might have coevolved with MglB Ct extension. Interestingly, MglB Ct negatively charged extension is conserved in all major bacterial phyla. Positively charged residues were absent in α5 helix of SofG (Figure 3.11 F). Based on these results, we proposed MglB C-terminal extension does not interact with SofG. SofG has an extra C-terminal extension of 40 amino acids beyond α5 helix of MglA predicted to form 2 helices. This extension might also be hindering the interaction of SofG and MglB C-terminal extension.

To substantiate this, we checked the GTPase activity of SofG in the presence of MglB and $MglB^{Ct}$. Interestingly we found GTPase activity of SofG in the presence of MglB and $MglB^{Ct}$ were similar (Figure 3.11 E). However, in MglA GTP hydrolysis was lower in the presence of $MglB^{Ct}$ as compared to MglB (Baranwal et al., unpublished). Hence, we conclude that MglB acts only as a GAP for SofG while it acts as both GAP and GEF for MglA.

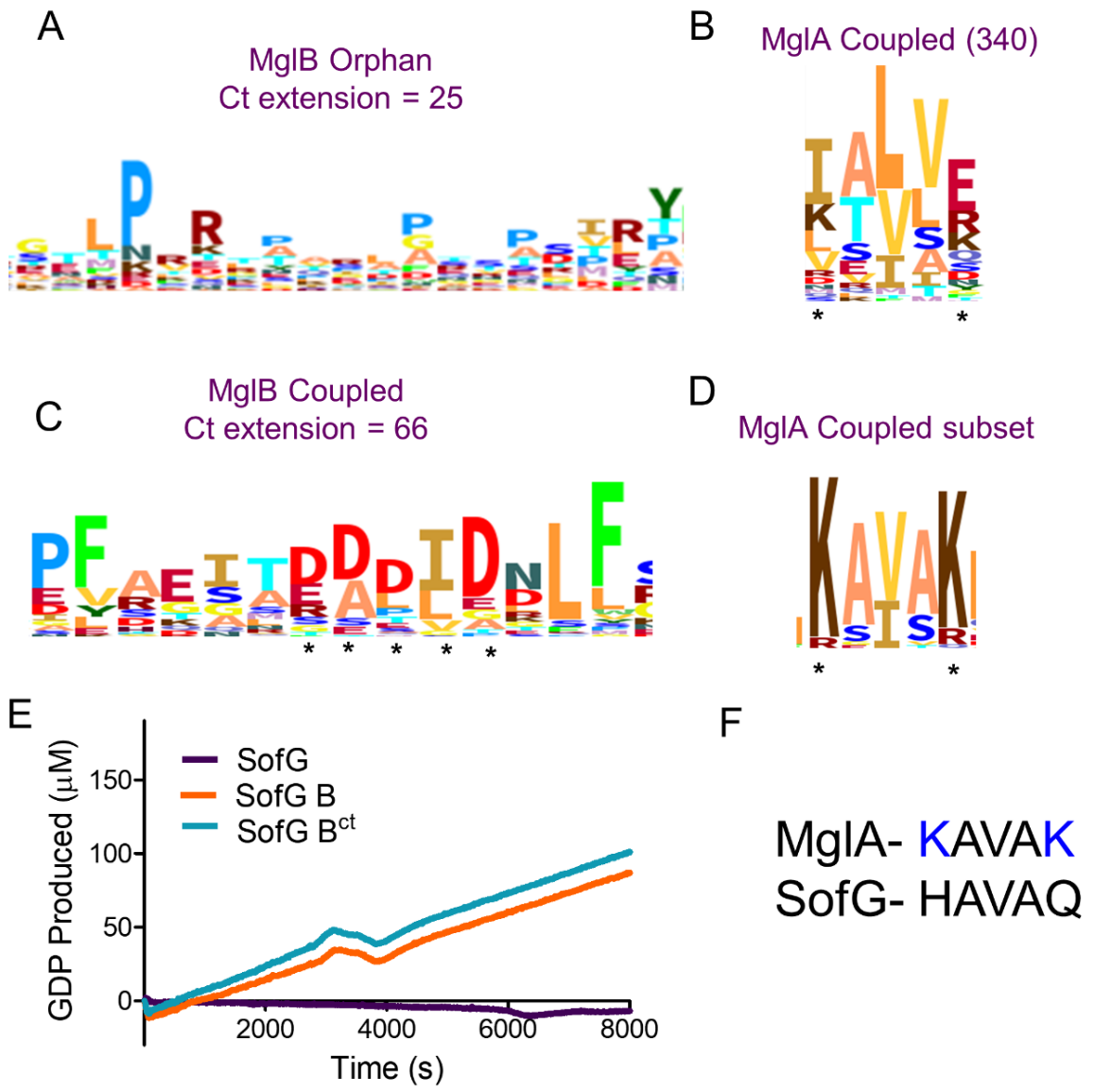

Figure 3.11. α5-helix of MglA is co-evolved with MglB Ct extension

A. Ct extension of MglB orphan is proline rich and lacks negatively charged residues **B.** Conservation of α5-helix of all MglA sequences coupled with MglB **C.** Negatively charged amino acids are conserved in MglB coupled Ct extension **D**. Conservation of α5 helix of MglA sequences coupled with MglB sequences having negatively charged amino acids. **E.** GTPase activity of SofG in presence of MglB (n=2; N=1) and $MglB^{Ct}$ (n=3; N=1) is similar. SofG (violet), SofG with MglB (orange) and SofG with $MglB^{Ct}$ **F.** α5-helix SofG does not have positively charged residues.

Chapter 4. Discussion

Biochemical characterization of the prokaryotic small Ras-like GTPase SofG

Purification optimization of SofG was challenging as SofG precipitates after elution. To reduce precipitation, purification was tried with different purification buffers in combination with various purification techniques. Finally, purification of SofG was optimized. SofG sufficient for biochemical characterization was purified without addition of GDP, which was not achieved before (Birjeet Singh, MS thesis, 2016; Sonal Lagad, MS thesis, 2017). Despite optimization, the final protein yield obtained is 20-30-fold less than other proteins (MglA and MglB) which I worked in my 5th year. For characterization of SofG, amount of protein required was massive as simple activity assay also required a final concentration of 10 µM of protein. Because of low yield and large amount protein required, extensive biochemical characterization of SofG is not reported till date.

Based on our experiments, we show that SofG is well folded and monomeric. Some GTPase having C-terminal extension forms higher order oligomers in presence of nucleotide (Zhang et al., 2001). However, nucleotide does not affect the oligomeric status of SofG, and it is monomeric upon addition of GDP or GTP. SofG binds to GDP and GTP, and nucleotide binding increases stability of protein. Intrinsic GTP hydrolysis rates of SofG and MglA were negligible. Small GTPases have very low intrinsic activity which gets stimulated in presence of GAP. Our results indicate SofG is a bonafide small GTPase. MglB stimulates GTP hydrolysis of MglA by approximately 35-fold, GAP activity of MglB plays a key role in determining cell polarity. GTPase activity of SofG is essential for polar localization of PilB and PilT. For active GTP hydrolysis and polarity, GAP is required for SofG.

MglB has dual specificity towards MglA and SofG

Sequence analysis indicated that MglB can potentially function as GAP for SofG (discussed in detail in results). GTPase activity of SofG increased 20-fold in presence of MglB. MglA and SofG have identical G motif and catalytic residues. GTP hydrolysis of MglA^{Q} and SofG^{Q} (active site mutant) was severely reduced in the presence of MglB. GTP hydrolysis of SofG and MglA were affected more than 10-fold in the presence of MglB^{G} (interface mutant). Since the same mutation at the MglAB interface

affects the activity and hence potentially the interaction between MglB and the GTPase in both MglA and SofG, the mode of interaction of MglB with both MglA and SofG is expected to be similar. Since the catalytic motifs are also conserved, they might have the same mechanism of GAP activity. Interestingly one of the differences in the mechanism of action between MglA and SofG interaction with MglB is that MglB does not function as a GEF for SofG and did not interact with it in the GDP-bound conformation.

Since MglB acts as a GAP for both MglA and SofG, it is possible that MglB contributes to the crosstalk between the two GTPases within the cell, during regulation of cell polarity. This prompted us to ask if GTPase regulators (GAP, GEF) can act on two different GTPases. Literature was checked for the reports where GTPase regulators act on more than one GTPase. Eukaryotic GAPs and GEFs interact with multiple GTPases which occur in common signalling pathways. Some examples from literature are summarized in table 4.1.

Table 4.1. List of GTPase regulators that act on multiple GTPases

	Effector	Activity	GTPase	Reference
1	Dock10	GEF	Rac1, Cdc42, Rac3, Rac2, RhoF and RhoG	(Ruiz-Lafuente et al., 2015)
2	SynGAP	GAP	Ras and Rap	(Pena et al., 2008)
3	CenA	GAP	Rab 6, Rab 2 and Rab 4	(Cuif et al., 1999)
4	ELMOD2	GAP	Arl2 and Arf	(Bowzard et al., 2007)
5	CAPRI	GAP	Ras and Rap	(Dai et al., 2011)
6	Rap1GAP	GAP	Di-Ras 1 and Di-Ras 2	(Gasper et al., 2010)
7	ARAP3	GAP	Arf 6, Arf 5 and RhoA	(Bao et al., 2016)
8	Gyp1p	GAP	Ypt1p, Ypt7p, and Ypt51p	(Du et al., 1998)
9	Rasa3	GAP	Ras and Rap1	(Kupzig et al., 2009)
10	R6IP1	GAP	Rab6 and Rab 11	(Miserey-Lenkei et al., 2007)
11	Dock6	GEF	Rac1 and Cdc42	(Miyamoto et al., 2007)
12	VPS9	GEF	Rab32 and Rab38	(Ohbayashi et al., 2012)

Discovery of a novel small Ras-like GTPase motif in prokaryotes

The most prominent feature of MglAB structure is the β screw movement in MglA. β screw rotation is essential for interaction with MglB. Sequence analysis led to the discovery of a novel prokaryotic G-motif which is important for MglB binding (part of the β-strand that undergoes rotation). In addition, the aspartate of Walker B motif conserved in most ATPases and GTPases was discovered to be part of this novel motif. G3 motif of MglA family lack conserved asparate, which is part of G3 motif in small GTPase family. Bifurcation of G3 motif in MglA family could be possibly to achieve tight regulation of GTPase activity stimulated by MglB. Walker B aspartate was mutated to alanine in MglA ($MglA^D$). GTPase activity $MglA^D$ was drastically reduced in the presence of MglB.This suggests that the β screw movement is an essential feature of catalytic mechanism of prokaryotic small Ras-like GTPases, since it is required for i) oriening catalytic arginine, and ii) for orienting the aspartate that coordinates the water bound to Mg^{2+}.

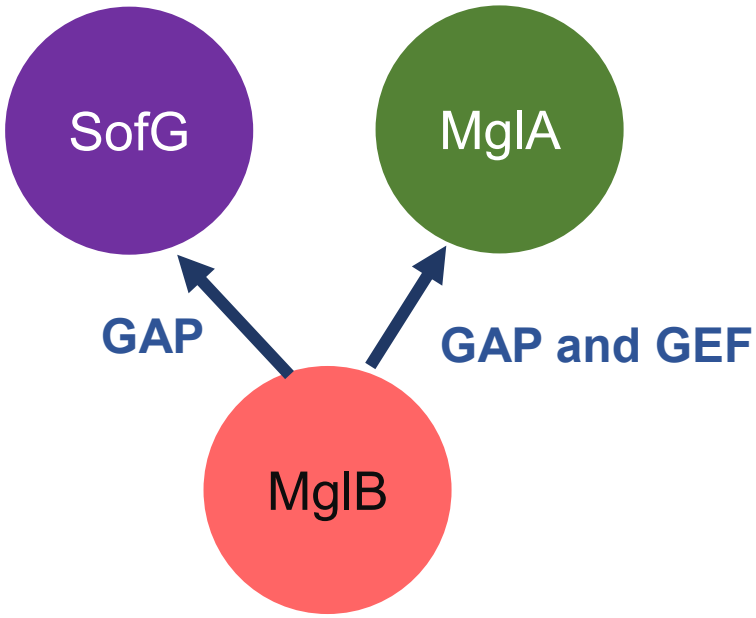

Figure 4.1 Schematic representation of MglB interaction toward SofG and MglA

Chapter 5. Conclusion and Future Perspectives

To elucidate the molecular mechanism of cell polarity regulation driven by MglA and SofG (small Ras-like GTPase) in *Myxococcus xanthus,* SofG purification was optimized, to obtain sufficient yield for biochemical and structural characterization. SofG is homogenous and monomeric in solution, GDP and GTP addition does not affect the oligomeric status of SofG. SofG is well folded and binds to GDP and GTP. GDP binding increases the stability of SofG and thus helps to reduce precipitation during purification. Intrinsic GTP hydrolysis rate of SofG is negligible. To identify GAP, we performed sequence analysis of MglA and MglB like proteins in prokaryotes. Our sequence analysis results indicate that MglB can potentially activate GTP hydrolysis of SofG. We experimentally showed that MglB stimulates GTP hydrolysis rate of SofG by approximately 20 fold. Using mutational analysis, we have shown that GAP mechanism of MglB is similar for SofG and MglA. MglB functions as GAP and GEF for MglA, while MglB acts as the GAP only for SofG. GDP bound SofG does not interact with MglB. Since MglB is a common GAP for both the GTPases, it could potentially mediate crosstalk between MglA and SofG.

Sequence analysis revealed co-evolution of i) MglA and MglB interface residues ii) negatively charged MglB Ct-helix with α5 helix of MglA. Sequence analysis also led to the discovery of novel catalytic motif in prokaryotes. Walker B aspartate which is part of canonical G3 motif in small GTPases was part of this newly identified motif. This was further validated by mutating aspartate to alanine in prototypic MglA. The mutation did not affect GTP binding, but GTP hydrolysis was affected. Since the role of MglA and MglB are not known in other organisms, our studies bring out common features of these proteins and validated through extensive biochemical studies.

We have qualitatively shown binding of SofG to nucleotide and MglB. To get information about binding affinity, I will explore quantitative interaction assays like MST and fluorescence anisotropy. Similar experiments need to be done for characterization of MglA and MglB mutants. Crystallization of SofG with different nucleotides and with MglB is also a future goal. Long term goal of this project is to understand the interaction of MglA and SofG with other effectors like PilB, PilT, and RomR.

Chapter 6. References:

Bao, H., Li, F., Wang, C., Wang, N., Jiang, Y., Tang, Y., Wu, J., and Shi, Y. (2016). Structural Basis for the Specific Recognition of RhoA by the Dual GTPase-activating Protein ARAP3. J. Biol. Chem. *291*, 16709–16719.

Bishop, A.L., and Hall, A. (2000). Rho GTPases and their effector proteins. Biochem. J. *348 Pt 2*, 241–255.

Bos, J.L., Rehmann, H., and Wittinghofer, A. (2007). GEFs and GAPs: critical elements in the control of small G proteins. Cell *129*, 865–877.

Bourne, H., David, and McCormick, F. The GTPase superfamily: conserved structure.

Bowzard, J.B., Cheng, D., Peng, J., and Kahn, R.A. (2007). ELMOD2 is an Arl2 GTPase-activating protein that also acts on Arfs. J. Biol. Chem. *282*, 17568–17580.

Bulyha, I., Lindow, S., Lin, L., Bolte, K., Wuichet, K., Kahnt, J., van der Does, C., Thanbichler, M., and Søgaard-Andersen, L. (2013). Two small GTPases act in concert with the bactofilin cytoskeleton to regulate dynamic bacterial cell polarity. Dev. Cell *25*, 119–131.

Cherfils, J., and Zeghouf, M. (2013). Regulation of small GTPases by GEFs, GAPs, and GDIs. Physiol. Rev. *93*, 269–309.

Clamp, M., Cuff, J., Searle, S.M., and Barton, G.J. (2004). The Jalview Java alignment editor. Bioinformatics *20*, 426–427.

Colicelli, J. (2004). Human RAS superfamily proteins and related GTPases. Sci STKE *2004*, RE13.

Crooks, G.E., Hon, G., Chandonia, J.M., and Brenner, S.E. (2004). WebLogo: a sequence logo generator. Genome Res. *14*, 1188–1190.

Cuif, M.H., Possmayer, F., Zander, H., Bordes, N., Jollivet, F., Couedel-Courteille, A., Janoueix-Lerosey, I., Langsley, G., Bornens, M., and Goud, B. (1999).

Characterization of GAPCenA, a GTPase activating protein for Rab6, part of which associates with the centrosome. EMBO J. *18*, 1772–1782.

Dai, Y., Walker, S.A., de Vet, E., Cook, S., Welch, H.C.E., and Lockyer, P.J. (2011). Ca2+-dependent monomer and dimer formation switches CAPRI Protein between Ras GTPase-activating protein (GAP) and RapGAP activities. J. Biol. Chem. *286*, 19905–19916.

Davis, B.M., and Waldor, M.K. (2013). Establishing polar identity in gram-negative rods. Curr. Opin. Microbiol. *16*, 752–759.

Du, L.L., Collins, R.N., and Novick, P.J. (1998). Identification of a Sec4p GTPase-activating protein (GAP) as a novel member of a Rab GAP family. J. Biol. Chem. *273*, 3253–3256.

Edgar, R.C. (2004). MUSCLE: multiple sequence alignment with high accuracy and high throughput. Nucleic Acids Res. *32*, 1792–1797.

Faure, L.M., Fiche, J.-B., Espinosa, L., Ducret, A., Anantharaman, V., Luciano, J., Lhospice, S., Islam, S.T., Tréguier, J., Sotes, M., et al. (2016). The mechanism of force transmission at bacterial focal adhesion complexes. Nature *539*, 530–535.

Fu, G., Bandaria, J.N., Le Gall, A.V., Fan, X., Yildiz, A., Mignot, T., Zusman, D.R., and Nan, B. (2018). MotAB-like machinery drives the movement of MreB filaments during bacterial gliding motility. Proc. Natl. Acad. Sci. USA *115*, 2484–2489.

Gasper, R., Sot, B., and Wittinghofer, A. (2010). GTPase activity of Di-Ras proteins is stimulated by Rap1GAP proteins. Small GTPases *1*, 133–141.

Gerwert, K., Mann, D., and Kötting, C. (2017). Common mechanisms of catalysis in small and heterotrimeric GTPases and their respective GAPs. Biol. Chem. *398*, 523–533.

Goitre, L., Trapani, E., Trabalzini, L., and Retta, S.F. (2014). The Ras superfamily of small GTPases: the unlocked secrets. Methods Mol. Biol. *1120*, 1–18.

Hall, A. (1998). Rho GTPases and the actin cytoskeleton. Science *279*, 509–514.

Hartzell, P., and Kaiser, D. (1991). Function of MglA, a 22-kilodalton protein essential for gliding in Myxococcus xanthus. J. Bacteriol. *173*, 7615–7624.

Iden, S., and Collard, J.G. (2008). Crosstalk between small GTPases and polarity proteins in cell polarization. Nat. Rev. Mol. Cell Biol. *9*, 846–859.

Jakovljevic, V., Leonardy, S., Hoppert, M., and Søgaard-Andersen, L. (2008). PilB and PilT are ATPases acting antagonistically in type IV pilus function in Myxococcus xanthus. J. Bacteriol. *190*, 2411–2421.

Kaimer, C., Berleman, J.E., and Zusman, D.R. (2012). Chemosensory signaling controls motility and subcellular polarity in Myxococcus xanthus. Curr. Opin. Microbiol. *15*, 751–757.

Keilberg, D., and Søgaard-Andersen, L. (2014). Regulation of bacterial cell polarity by small GTPases. Biochemistry *53*, 1899–1907.

Kiianitsa, K., Solinger, J.A., and Heyer, W.-D. (2003). NADH-coupled microplate photometric assay for kinetic studies of ATP-hydrolyzing enzymes with low and high specific activities. Anal. Biochem. *321*, 266–271.

Kupzig, S., Bouyoucef-Cherchalli, D., Yarwood, S., Sessions, R., and Cullen, P.J. (2009). The ability of GAP1IP4BP to function as a Rap1 GTPase-activating protein (GAP) requires its Ras GAP-related domain and an arginine finger rather than an asparagine thumb. Mol. Cell. Biol. *29*, 3929–3940.

Leipe, D.D., Wolf, Y.I., Koonin, E.V., and Aravind, L. (2002). Classification and evolution of P-loop GTPases and related ATPases. J. Mol. Biol. *317*, 41–72.

Letunic, I., Goodstadt, L., Dickens, N.J., Doerks, T., Schultz, J., Mott, R., Ciccarelli, F., Copley, R.R., Ponting, C.P., and Bork, P. (2002). Recent improvements to the SMART domain-based sequence annotation resource. Nucleic Acids Res. *30*, 242–244.

Levine, T.P., Daniels, R.D., Wong, L.H., Gatta, A.T., Gerondopoulos, A., and Barr, F.A. (2013). Discovery of new Longin and Roadblock domains that form platforms for small GTPases in Ragulator and TRAPP-II. Small GTPases *4*, 62–69.

Li, H.-Y., Cao, K., and Zheng, Y. (2003). Ran in the spindle checkpoint: a new function for a versatile GTPase. Trends Cell Biol. *13*, 553–557.

McLoon, A.L., Wuichet, K., Häsler, M., Keilberg, D., Szadkowski, D., and Søgaard-Andersen, L. (2016). MglC, a Paralog of Myxococcus xanthus GTPase-Activating Protein MglB, Plays a Divergent Role in Motility Regulation. J. Bacteriol. *198*, 510–520.

Miertzschke, M., Koerner, C., Vetter, I.R., Keilberg, D., Hot, E., Leonardy, S., Søgaard-Andersen, L., and Wittinghofer, A. (2011). Structural analysis of the Ras-like G protein MglA and its cognate GAP MglB and implications for bacterial polarity. EMBO J. *30*, 4185–4197.

Miserey-Lenkei, S., Waharte, F., Boulet, A., Cuif, M.-H., Tenza, D., El Marjou, A., Raposo, G., Salamero, J., Héliot, L., Goud, B., et al. (2007). Rab6-interacting protein 1 links Rab6 and Rab11 function. Traffic *8*, 1385–1403.

Mishra, A.K., and Lambright, D.G. (2016). Invited review: Small GTPases and their GAPs. Biopolymers *105*, 431–448.

Miyamoto, Y., Yamauchi, J., Sanbe, A., and Tanoue, A. (2007). Dock6, a Dock-C subfamily guanine nucleotide exchanger, has the dual specificity for Rac1 and Cdc42 and regulates neurite outgrowth. Exp. Cell Res. *313*, 791–804.

Ohbayashi, N., Yatsu, A., Tamura, K., and Fukuda, M. (2012). The Rab21-GEF activity of Varp, but not its Rab32/38 effector function, is required for dendrite formation in melanocytes. Mol. Biol. Cell *23*, 669–678.

Pena, V., Hothorn, M., Eberth, A., Kaschau, N., Parret, A., Gremer, L., Bonneau, F., Ahmadian, M.R., and Scheffzek, K. (2008). The C2 domain of SynGAP is essential for stimulation of the Rap GTPase reaction. EMBO Rep. *9*, 350–355.

Qiu, B., Zhang, K., Wang, S., and Sun, F. (2014). C-terminal motif within Sec7 domain regulates guanine nucleotide exchange activity via tuning protein conformation. Biochem. Biophys. Res. Commun. *446*, 380–386.

Rajalingam, K., Schreck, R., Rapp, U.R., and Albert, S. (2007). Ras oncogenes and their downstream targets. Biochim. Biophys. Acta *1773*, 1177–1195.

Ruiz-Lafuente, N., Alcaraz-García, M.-J., García-Serna, A.-M., Sebastián-Ruiz, S., Moya-Quiles, M.-R., García-Alonso, A.-M., and Parrado, A. (2015). Dock10, a

Cdc42 and Rac1 GEF, induces loss of elongation, filopodia, and ruffles in cervical cancer epithelial HeLa cells. Biol. Open *4*, 627–635.

Schumacher, D., and Søgaard-Andersen, L. (2017). Regulation of Cell Polarity in Motility and Cell Division in Myxococcus xanthus. Annu. Rev. Microbiol. *71*, 61–78.

Senisterra, G.A., Markin, E., and Yamazaki, K. (2006). Screening for ligands using a generic and high-throughput light-scattering-based assay. Journal of ….

Serra, S., and Morgante, L. (1980). [Method of determination of proteins with Coomassie brilliant blue G 250. I. General characteristics and comparative analysis with the biuret method and Lowry's method]. Boll Soc Ital Biol Sper *56*, 160–165.

Simanshu, D.K., Nissley, D.V., and McCormick, F. (2017). RAS proteins and their regulators in human disease. Cell *170*, 17–33.

Takai, Y., Sasaki, T., and Matozaki, T. (2001). Small GTP-binding proteins. Physiol. Rev. *81*, 153–208.

van den Ent, F., and Löwe, J. (2006). RF cloning: a restriction-free method for inserting target genes into plasmids. J Biochem Biophys Methods *67*, 67–74.

Vetter, I.R., and Wittinghofer, A. (2001). The guanine nucleotide-binding switch in three dimensions. Science *294*, 1299–1304.

Wennerberg, K., Rossman, K.L., and Der, C.J. (2005). The Ras superfamily at a glance. J. Cell Sci. *118*, 843–846.

Wheeler, T.J., Clements, J., and Finn, R.D. (2014). Skylign: a tool for creating informative, interactive logos representing sequence alignments and profile hidden Markov models. BMC Bioinformatics *15*, 7.

Wittinghofer, A., and Vetter, I.R. (2011). Structure-function relationships of the G domain, a canonical switch motif. Annu. Rev. Biochem. *80*, 943–971.

Wu, X., Bradley, M.J., Cai, Y., Kümmel, D., De La Cruz, E.M., Barr, F.A., and Reinisch, K.M. (2011). Insights regarding guanine nucleotide exchange from the structure of a DENN-domain protein complexed with its Rab GTPase substrate. Proc. Natl. Acad. Sci. USA *108*, 18672–18677.

Wuichet, K., and Søgaard-Andersen, L. (2014). Evolution and diversity of the Ras superfamily of small GTPases in prokaryotes. Genome Biol. Evol. *7*, 57–70.

Zhang, B., Gao, Y., Moon, S.Y., Zhang, Y., and Zheng, Y. (2001). Oligomerization of Rac1 gtpase mediated by the carboxyl-terminal polybasic domain. J. Biol. Chem. *276*, 8958–8967.

Zhang, Y., Franco, M., Ducret, A., and Mignot, T. (2010). A bacterial Ras-like small GTP-binding protein and its cognate GAP establish a dynamic spatial polarity axis to control directed motility. PLoS Biol. *8*, e1000430.

Zhang, Y., Guzzo, M., Ducret, A., Li, Y.-Z., and Mignot, T. (2012). A dynamic response regulator protein modulates G-protein-dependent polarity in the bacterium Myxococcus xanthus. PLoS Genet. *8*, e1002872.